Manuscript # acp-2018-904

Responses to Reviewer #1

This study concerns the climate response of black carbon (BC) emissions in a fully- coupled climate model. The study is motivated by the potential for BC emissions reductions, and the authors evaluate the non-linearity of emission perturbations and the transient response. As BC has received attention from a policy-perspective to reduce global warming (e.g. CCAC and the Arctic Council), investigating possible non- linearities in emission perturbations and the transient response of BC is important and highly relevant for ACP.

We thank the reviewer for all the insightful comments. Below, please see our point-by-point responses (in blue) to the specific comments and suggestions and the changes that have been made to the manuscript to take into account all the comments raised here.

Unfortunately, I think the study fails to answer these questions. Since the authors do not find any significant climate change from present-day BC emissions, the authors conclude that BC emission cuts may not be detectable and that the climate impact of BC should be expressed directly in terms of emissions.

Indeed, we do conclude that there may be no detectable surface **temperature** change impacts from present-day BC over much of the world (note we do not conclude there are no *climate* impacts, since BC will impact other variables). Note, our specific wording on this point:

> *These results indicate that even substantial BC emissions reductions from current levels may lead to detectable surface temperature changes for only limited regions of the globe. (line 560)*

Which we believe accurately reflects our findings and does, indeed, address the questions raised by many on this topic (albeit from one model of course).

We did not intend to say that the impact of BC should be expressed as emissions, we apologize for the misunderstanding. This portion of the discussion section has been re-written to clarify as:

> *We suggest that impacts of BC on climate should be expressed directly in terms of impacts per unit emissions (e.g. table 1), and not only relative to forcing given the complex relationship between BC climatic impacts and top of the atmosphere forcing. In addition, BC impacts should be re-evaluated using coupled models, and provided with measures of response variability, such as standard deviation.*

First; Do the authors mean that we cannot say anything about the climate impact of BC? I would argue that emissions are not climate impacts. As this paper is clearly motivated by policy-relevant questions, I am confused about what the authors are trying to conclude.

Response:

We can indeed say something about BC impacts on climate. We can say that, over most of the globe, BC impacts on surface temperature are very small.

Second; I agree that cutting BC emissions would not be detectable on a thermostat in the real world. As a matter of fact; few things would, except radical changes like cutting CO2-emissions to zero. Is this relevant? As researchers, we must use models (this is why we use them) to provide our best estimate on the climate impact of e.g. cutting BC emissions, and then it is up to the policy-makers to decide if it is worth it in terms of costs, feasibility, co-emitted species etc.

Response:

This statement by the reviewer that only changes such as cutting CO2 emissions to zero would be detectable is not correct. For example, differences in climate variables between a RCP8.5 and RCP4.5 scenario begin to be statistically detectable as early as 25–30 years after scenarios diverge (Tebaldi and Friedlingstein 2013), well before CO_2 emissions are zero. Cutting SO_2 emissions to zero, for example, also leads to detectable changes in surface temperature over much of the world (Baker et al. 2015). However, the impact of reducing BC emissions on surface temperature is much smaller due, in part, to the counteracting cooling and warming effects of fast feedbacks that are only present in coupled model simulations (as demonstrated in a number of models recently by Stjern et al. 2017).

Note that we did not provide any recommendation on the desirability of reducing BC emissions. We have, however, found in our simulations that the impact of reducing BC emissions, even to the point of eliminating all anthropogenic emissions, is small and statistically undetectable across most of the globe.

Third; the simulating period for these runs are too short to make these conclusions. If the simulation period was long enough, I argue that the authors would 1) be able to detect a signal from present-day emissions and 2) quantify the non-linearity of different emissions perturbations. Are the temperature sensitivities in Figure 8 significantly different from each other? The authors refer to natural variability as error bars, which I find a bit odd.

Response:

The runs were as long as computationally feasible (e.g. multiple 100-year coupled simulations), and our results are provided with the uncertainty

estimates derived from these simulations. To reduce uncertainty further, a far longer set of runs would be required since noise in this case would reduce as 1/sqrt(Neff), where Neff equals the simulation length divided by the correlation time-scale for the processes in question.

We have added statistical tests in Figure 8 and Table 2 as shown below and modified the manuscript adding these tests.

Note that we did not “refer to natural variability as error bars”, the error bars represent one standard deviation of the signals derived from our runs to indicate uncertainty. We do, however, conclude that the root of this variability in our signal likely stems from internal variability in the model due to the statistical properties we find in our analysis.

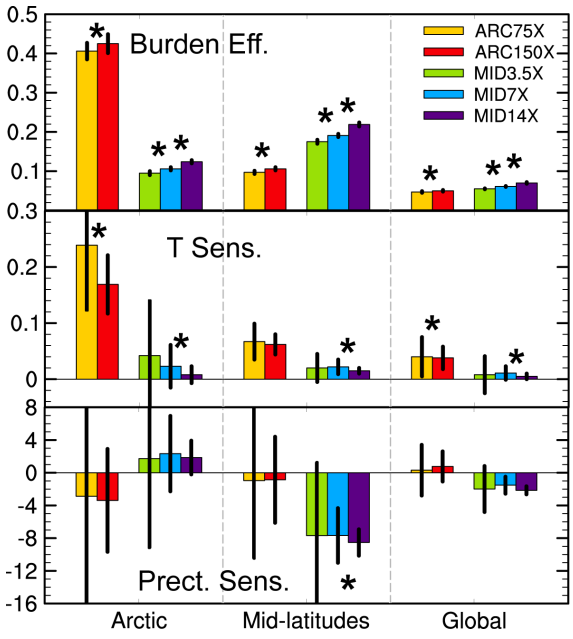

Figure 8. Burden efficiencies, temperature and precipitation sensitivities over the Arctic, mid-latitudes and the whole globe for ARC75X, ARC150X, MID3.5X, MID7X and MID14X. Burden efficiencies, temperature sensitivity and precipitation sensitivity are calculated as changes in regional mean BC column burden, surface temperature and total precipitation rate divided by changes in global total BC emissions between perturbed and PD simulations, respectively. Error bars represent 1-σ for 80-annual means. Asterisk between two bars (ARC75X/ARC150X, MID3.5X/MID7X, and MID7X/MID14X) indicates statistically significant changes with 95% confidence from a two-tailed Student’s t test.

Table 2. BC burden, DRE, CRE, and snow/ice-albedo forcing efficiencies, T sensitivity and P sensitivity over the Arctic (60–90°N), mid-latitudes (28–60°N) and the globe between perturbed (ARC75X/ARC150X/MID3.5X/MID7X/MID14X) and PD simulations. 1-σ for 80-annual means is shown in the parentheses. Bold values between two simulations (ARC75X/ARC150X, MID3.5X/MID7X, and MID7X/MID14X) indicates statistically significant changes with 95% confidence from a two-tailed Student's t test.

		ARC75X	ARC150X			MID3P5X	MID7X	MID14X
		Burden Eff. (mg m^{-2} (Tg yr^{-1})$^{-1}$)						
60–90°N		**0.406 (±0.021)**	**0.425 (±0.024)**			**0.095 (±0.005)**	**0.106 (±0.004)**	**0.124 (±0.004)**
28–60°N		**0.097 (±0.004)**	**0.106 (±0.004)**			**0.175 (±0.005)**	**0.191 (±0.004)**	**0.219 (±0.005)**
Global		**0.047 (±0.002)**	**0.050 (±0.002)**			**0.055 (±0.001)**	**0.061 (±0.001)**	**0.070 (±0.002)**
		DRE Eff. (W m^{-2} (Tg yr^{-1})$^{-1}$)						
60–90°N		**0.346 (±0.036)**	**0.312 (±0.031)**			**0.146 (±0.014)**	**0.140 (±0.009)**	**0.137 (±0.006)**
28–60°N		**0.069 (±0.005)**	**0.066 (±0.003)**			**0.129 (±0.006)**	**0.120 (±0.004)**	**0.112 (±0.003)**
Global		**0.038 (±0.003)**	**0.035 (±0.003)**			**0.051 (±0.003)**	**0.048 (±0.002)**	**0.046 (±0.001)**
		CRE Eff. (W m^{-2} (Tg yr^{-1})$^{-1}$)						
60–90°N		**–0.533 (±0.232)**	**–0.303 (±0.078)**			–0.091 (±0.166)	**–0.111 (±0.046)**	**–0.015 (±0.029)**
28–60°N		0.010 (±0.222)	–0.037 (±0.067)			**0.070 (±0.203)**	**–0.152 (±0.043)**	**0.129 (±0.035)**
Global		**–0.028 (±0.071)**	**–0.017 (±0.043)**			0.013 (±0.058)	**–0.061 (±0.025)**	**0.035 (±0.010)**
		Snow/ice-albedo Eff. (W m^{-2} (Tg yr^{-1})$^{-1}$)						
60–90°N		**0.151 (±0.011)**	**0.099 (±0.006)**			**0.030 (±0.003)**	**0.026 (±0.002)**	**0.020 (±0.002)**
28–60°N		**0.013 (±0.003)**	**0.010 (±0.002)**			**0.011 (±0.002)**	**0.009 (±0.001)**	**0.007 (±0.001)**
Global		**0.012 (±0.001)**	**0.008 (±0.001)**			**0.004 (±0.001)**	**0.003 (±0.000)**	**0.003 (±0.000)**
		T Sensitivity (K (Tg yr^{-1})$^{-1}$)						
60–90°N		**0.239 (±0.116)**	**0.169 (±0.052)**			0.042 (±0.098)	**0.023 (±0.038)**	**0.008 (±0.015)**
28–60°N		0.067 (±0.032)	0.062 (±0.018)			0.020 (±0.025)	**0.022 (±0.013)**	**0.015 (±0.005)**
Global		**0.040 (±0.035)**	**0.038 (±0.020)**			0.008 (±0.033)	**0.011 (±0.012)**	**0.005 (±0.005)**
		P Sensitivity (μm day-1 (Tg yr^{-1})$^{-1}$)						
60–90°N		–2.88 (±13.39)	–3.38 (±6.29)			1.73 (±10.85)	2.34 (±4.61)	1.86 (±2.06)
28–60°N		–0.96 (±9.45)	–0.86 (±5.26)			–7.69 (±8.90)	**–7.67 (±3.34)**	**–8.53 (±1.61)**
Global		0.31 (±3.10)	0.77 (±1.84)			–1.99 (±2.81)	–1.52 (±1.04)	–2.15 (±0.49)

The most important finding in this study, I think, is the short transient response of 2-3 years and the lack of a long-term response that the authors find for BC. This contradicts the much-used study by Boucher and Reddy (2007) where it is shown that BC both has a short-term response and a long-term response (ocean). If this is true it will be important for policy-makers, as a rapid BC mitigation will not be crucial for reaching e.g. the 2-degree target and can be delayed for some time. Physically, this means that BC emissions mostly influences the boundary layer over land surface, and do not warm the ocean

due to a stabilization of the marine stratocumulus clouds. Would this be specific or sensitive to the model and the cloud scheme? In Boucher and Reddy (2007), they use an impulse temperature response function with both a short-term and a long term. How certain are the authors that there is no long-term response? In L404 you state that 'by our observation that there is no detectable long-term trend after the initial transient period'. This is a bit vague. Can you perform a hypothesis test to see if there is no long-term trend? But, again, the simulation period is too short to estimate any long-term responses.

Response:

We note that Boucher and Reddy (2008), and much other previous work, use a GHG impulse response function for the BC response. This was an implicit assumption that the system responds similar to a BC impulse as to a GHG inputs. This is known not to be the case for aerosols in general, since their forcing is not uniformly distributed in space (e.g., the "geometric effect" as noted by Meinshausen et al. (2011) and Shindell (2014)). As we note in the text, a similar result for BC (for a global emission perturbation) was found by Sand et al. (2015).

We did indeed statistically test for a long-term response and we have amended the text to cite the result of our linear fit showing there is no long-term response. We have amended the text to indicate that, as the reviewer points out, that we can only conclude there is no significant response over a 100-year time horizon. We cannot draw conclusions for longer-time scales.

I suggest that the authors either extend their simulation period or significantly tone down their conclusions. But if the latter; I am not sure how much added value this study will provide. However, if the authors do extend their simulation period (yes, this will require some extra work), I think this study can be an important contribution to the field.

Response:

We disagree that it is necessary to extend the simulations to draw relevant conclusions. While it would be interesting to do so, it is not clear if the computational costs could be justified. 100-years is a standard length for model diagnoses of this sort (e.g. Baker et al. 2015) and provides sufficient statistics for analysis.

Reference:

Boucher, O. and Reddy, M. S.: Climate trade-off between black carbon and carbon dioxide emissions, Energ. Policy, 36, 193–200, doi:10.1016/j.enpol.2007.08.039, 2008.

Meinshausen, M., Smith, S. J., Calvin, K., Daniel, J. S., Kainuma, M. L. T., Lamarque, J.-F., Matsumoto, K., Montzka, S. A., Raper, S. C. B., Riahi, K., Thomson, A., Velders, G. J. M., and van Vuuren, D. P. P.: The RCP greenhouse gas concentrations and their extensions from 1765 to 2300, Climatic Change, 109, 213 – 241, doi:10.1007/s10584-011-0156-z, 2011.

Shindell, D.: Inhomogeneous forcing and transient climate sensitivity, Nat. Clim. Change, 4, 274 – 277, doi:10.1038/nclimate2136, 2014.

Sand, M., Iversen, T., Bohlinger, P., Kirkevåg, A., Seierstad, I., Seland, Ø., and Sorteberg, A: A standardized global climate model study showing unique properties for the climate response to black carbon aerosols, J. Climate., 28, 2512–2526, doi:10.1175/JCLI-D-14-00050.1, 2015.

Responses to Reviewer #2

This study investigated the regional climate responses, non-linearity, and short-term transient responses to BC emission. The topic is of interest and the method scientifically sounds.

We thank the reviewer for all the insightful comments. Below, please see our point-by-point responses (in blue) to the specific comments and suggestions and the changes that have been made to the manuscript, attempting to take into account all the comments raised here.

Major comments

1)There is no model evaluation in this study. How does the model in terms of the aerosol species or climate variables? Some statistical evaluations are useful to warrant the confidence in interpreting the model results.

Response:

Previous studies have extensively evaluated the CAM5 model simulations of concentration, deposition, vertical profile and optical properties of BC (Wang et al., 2013; Wang et al., 2015; Zhang et al., 2015a,b; Liu et al., 2016; Yang et al., 2017, 2018a,b)), as well as climate variables (Hurrell et al., 2013; Yang et al., 2016a,b). The model can simulate well the BC aerosol and climate variables in most regions of the globe, but was reported to underestimate BC concentrations over China (Yang et al., 2018a) and the Arctic (Wang et al., 2013) (although this earlier study used a different emissions dataset), implying a possible underestimate of climate responses to BC emissions in this study. We have added these texts in the methods section.

2) The authors mainly analyzed the results from the annual scale. Are there any substantial differences in a finer temporal scale, i.e., daily or monthly or seasonal?

Response:

Thanks for the suggestion. We have added Figures S2 and S3 as below to show the seasonal and monthly surface air temperature change. Since that the climate response and variability are normally longer than daily scale, we skipped the daily information. We have also added texts in the manuscript to illustrate the seasonal difference that “The seasonal mean surface air temperature responses present similar spatial patterns (Figure S2), but slightly different magnitudes (Figure S3). Over the Arctic, the warming due to Arctic BC emissions is weakest in boreal summer. This is because the smaller summer sea ice and snow fraction in the Arctic weakens BC snow/ice-albedo forcing. However, in the mid-latitudes, warming is strongest in boreal summer for both Arctic and mid-latitude BC emissions, because of stronger summer solar

insolation and, therefore, stronger BC heating in the atmosphere."

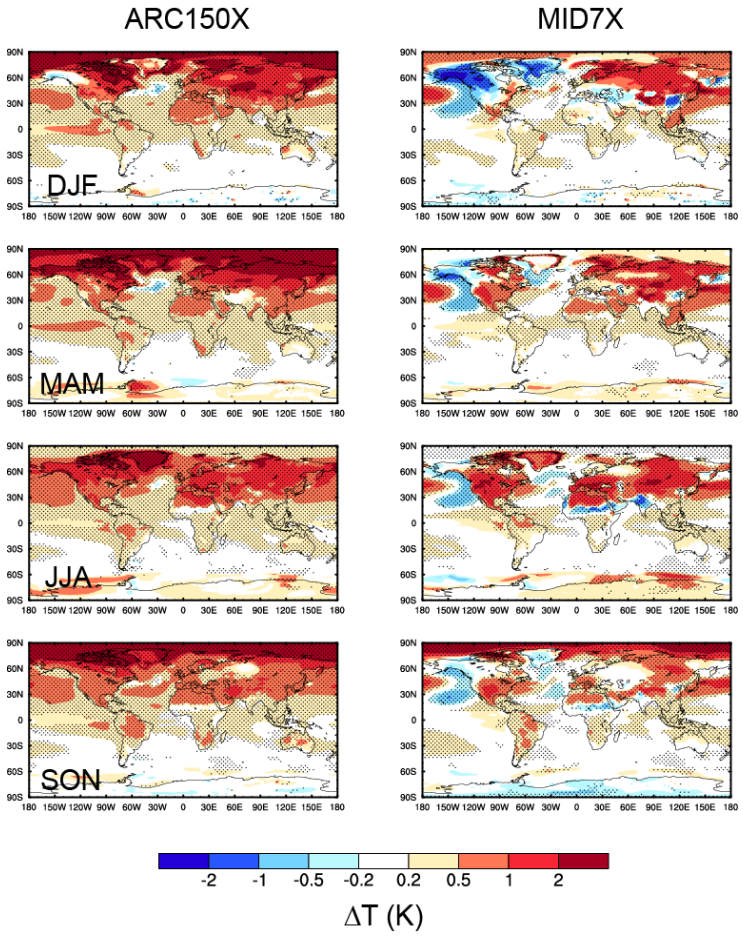

Figure S2. Spatial distribution of changes in December-January-February (DJF), March-April-May (MAM), June-July-August (JJA) and September-October-November (SON) (from top to bottom) mean surface air temperature (K) for ARC150X (left) and MID7X (right) compared to PD. The dotted areas indicate statistical significance with 95% confidence from a two-tailed Student's t test.

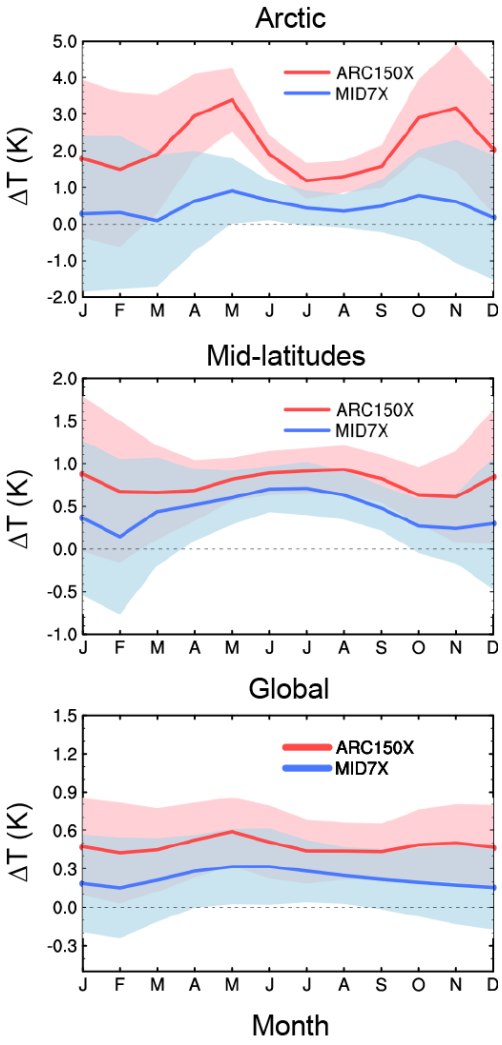

Figure S3. Changes in Arctic (top), mid-latitude (middle) and global (bottom) monthly mean surface temperature (K) for ARC150X/MID7X compared to PD.

Minor comments:

2)Line 283: due to their 30 times larger: how to get the value of 30?
Response:
Revised to “Mid-latitude emissions, however, are likely to have a larger present-day impact overall due to their 35 times larger preindustrial to present-day emission increase (2.874 Tg yr^{-1}) than Arctic emissions (0.082 Tg yr^{-1}).”

3) Figures 4-7: The captions need to be revised to explain the meaning of the dots. In Figure 2, it says that “The dotted areas in left panels indicate statistical significance with 95% confidence from a two-tailed Student’s t test.” Probably the dots in figures 4-7 share the same meaning. Please clarify.
Response:
Yes. Clarified in Figure 4-7.

4) Page 10, Line 194: Both mass and number of BC
Response:
CAM5 predicts both mass and number mixing ratios of aerosols, which requires both the mass and number emissions. That is why we mentioned here that “Both mass and number of BC emissions are perturbed proportionally.”

5) Line 273-274: from Figure 3, we can see some substantial changes in the south hemisphere. What does this mean? Were the emissions scaled in the south hemisphere as well?
Response:
We only scaled BC emissions in the Arctic and mid-latitudes of the Northern Hemisphere, respectively. Energy balance is not like the short-lived BC aerosol, which is mainly located near its sources. With the strong BC perturbation in the whole Arctic and mid-latitudes, energy balance will be changed not only in the regions where it is perturbed, but in the global scale, because the perturbation changes the latitudinal temperature gradient and therefore the poleward heat transport in both Northern and Southern Hemisphere.

6) Line 446-447: Large scale surface temperature from current-day BC emissions is statistically indistinguishable from zero. The authors’ statement is based on global scale. Since the variability is large, are there any features (i.e., larger change in some areas) in different locations?
Response:
Thanks for the suggestions. Yes, there are significant temperature changes regionally. “PD emissions produce statistically significant surface air temperature changes over only limited regions in the Northern Hemisphere. Decreased temperatures are found over eastern China, South Asia, North

Atlantic Ocean, and North American Arctic, partly due to cloud changes driven by BC rapid adjustments. Increased temperatures are found over the Tibetan Plateau, Greenland and high-latitude land regions likely because of the BC snow/ice-albedo effect". To make it clearer, we have also revised the text as "Although statistically significant surface temperature changes are found regionally, as mentioned above, large-scale global surface temperature change from current-day BC emissions is statistically indistinguishable from zero".

7) Line 522: BC direct radiative effects and snow/ice-albedo forcings have much larger signal to noise ratios: Could you please explain a bit more what the larger signal to noise ratio mean?

Response:

Changed to "aerosol burdens, BC direct radiative effects and snow/ice-albedo forcings have much larger signal to noise ratios, i.e. ratio of mean response to standard deviation (Table 1)"

Reference:

Hurrell, J. W., Holland, M. M., Gent, P. R., Ghan, S., Kay, J. E., Kushner, P. J., Lamarque, J. F., Large, W. G., Lawrence, D., Lindsay, K., Lipscomb, W. H., Long, M. C., Mahowald, N., Marsh, D. R., Neale, R. B., Rasch, P., Vavrus, S., Vertenstein, M., Bader, D., Collins, W. D., Hack, J. J., Kiehl, J., and Marshall, S. (2013), The Community Earth System Model A Framework for Collaborative Research, B. Am. Meteorol. Soc., 94, 1339–1360, doi:10.1175/BAMS-D-12-00121.1.

Liu, X., Easter, R. C., Ghan, S. J., Zaveri, R., Rasch, P., Shi, X., Lamarque, J.-F., Gettelman, A., Morrison, H., Vitt, F., Conley, A., Park, S., Neale, R., Hannay, C., Ekman, A. M. L., Hess, P., Mahowald, N., Collins, W., Iacono, M. J., Bretherton, C. S., Flan- ner, M. G., and Mitchell, D.: Toward a minimal representation of aerosols in climate models: description and evaluation in the Community Atmosphere Model CAM5, Geosci. Model Dev., 5, 709–739, doi:10.5194/gmd-5-709-2012, 2012.

Liu, X., Ma, P.-L., Wang, H., Tilmes, S., Singh, B., Easter, R. C., Ghan, S. J., and Rasch, P. J. (2016), Description and evaluation of a new four-mode version of the Modal Aerosol Module (MAM4) within version 5.3 of the Community Atmosphere Model, Geosci. Model Dev., 9, 505–522, doi:10.5194/gmd-9-505-2016.

Meinshausen, M., Raper, S. C. B., and Wigley, T. M. L.: Emulating coupled atmosphere-ocean and carbon cycle models with a simpler model, MAGICC6 – Part 1: Model description and calibration, Atmos. Chem. Phys., 11, 1417-1456, https://doi.org/10.5194/acp-11-1417-2011, 2011.

Shindell, D.T., 2014: Inhomogeneous forcing and transient climate

sensitivity. *Nature Clim. Change*, **4**, 274-277, doi:10.1038/nclimate2136

Tebaldi, C. and Friedlingstein, P., 2013. Delayed detection of climate mitigation benefits due to climate inertia and variability. *Proceedings of the National Academy of Sciences*, p.201300005.

Wang, H., Easter, R. C., Rasch, P. J., Wang, M., Liu, X., Ghan, S. J., Qian, Y., Yoon, J.-H., Ma, P.-L., and Vinoj, V.: Sensitivity of remote aerosol distributions to representation of cloud–aerosol interactions in a global climate model, Geosci. Model Dev., 6, 765-782, doi:10.5194/gmd-6-765-2013, 2013.

Wang, M., Larson, V., Ghan, S., Ovchinnikov, M., Schanen, D., Xiao, H., Liu, X., Guo, Z., and Rasch, P.: A multiscale modeling framework model (superparameterized CAM5) with a higher-order turbulence closure: Model description and low-cloud simulations, J. Adv. Model. Earth Syst., 7, 484–509, doi:10.1002/2014MS000375, 2015.

Yang, Y., Russell, L. M., Xu, L., Lou, S., Lamjiri, M. A., Somerville, R. C. J., Miller, A. J., Cayan, D. R., DeFlorio, M. J., Ghan, S. J., Liu, Y., Singh, B., Wang, H., Yoon, J.-H., and Rasch, P. J.: Impacts of ENSO events on cloud radiative effects in preindustrial conditions: Changes in cloud fraction and their dependence on interactive aerosol emissions and concentrations, J. Geophys. Res. Atmos., 121, 6321–6335, doi:10.1002/2015JD024503, 2016a.

Yang, Y., Russell, L. M., Lou, S., Lamjiri, M. A., Liu, Y., Singh, B., and Ghan, S. J.: Changes in Sea Salt Emissions Enhance ENSO Variability, J. Climate, 29, 8575–8588, doi:10.1175/JCLI-D-16-0237.1, 2016b.

Yang, Y., Wang, H., Smith, S. J., Ma, P.-L., and Rasch, P. J.: Source attribution of black carbon and its direct radiative forcing in China, Atmos. Chem. Phys., 17, 4319-4336, doi:10.5194/acp-17-4319-2017, 2017.

Yang, Y., Wang, H., Smith, S. J., Zhang, R., Lou, S., Qian, Y., Ma, P.-L., Rasch, P. J.: Recent intensification of winter haze in China linked to foreign emissions and meteorology, Sci. Rep., 8, 2107, doi:10.1038/s41598-018-20437-7, 2018a.

Yang, Y., Wang, H., Smith, S. J., Zhang, R., Lou, S., Yu, H., Li, C., and Rasch, P. J.: Source apportionments of aerosols and their direct radiative forcing and long-term trends over continental United States, Earth's Future, 6, 793–808, doi:10.1029/2018EF000859, 2018b.

Variability, timescales, and non-linearity in climate responses to black carbon emissions

Yang Yang[1*], Steven J. Smith[2*], Hailong Wang[1], Catrin M. Mills[1], Philip J. Rasch[1]

[1]Atmospheric Sciences and Global Change Division, Pacific Northwest National Laboratory, Richland, Washington, USA

[2]Joint Global Change Research Institute, Pacific Northwest National Laboratory, College Park, Maryland, USA

*Correspondence to yang.yang@pnnl.gov and ssmith@pnnl.gov

Abstract

Black carbon (BC) particles exert a potentially large warming influence on the Earth system. Reductions in BC emissions have attracted attention as a possible means to moderate near-term temperature changes. For the first time, we evaluate regional climate responses, non-linearity, and short-term transient responses to BC emission perturbations in the Arctic, mid-latitudes, and globally based on a comprehensive set of emission-driven experiments using the Community Earth System Model (CESM). Surface temperature responses to BC emissions are complex, with surface warming over land from mid-latitude BC perturbations partially offset by ocean cooling. Climate responses do not scale linearity with emissions. While stronger BC emission perturbations have a higher burden efficiency, their temperature sensitivity is lower. BC impacts temperature much faster than greenhouse gas forcing, with transient temperature responses in the Arctic and mid-latitudes approaching a quasi-equilibrium state with a timescale of 2–3 years. We find large variability in BC-induced climate changes due to background model noise. As a result, removing present-day BC emissions results in discernible surface temperature changes for only limited regions of the globe. In order to better understand the climatic impacts of BC emissions, both the drivers of non-linear responses and response variability need to be assessed across climate models.

Deleted: perturbing

Deleted: emission levels

Deleted: no

Deleted: net global-average

Deleted: signal

1. Introduction

Black carbon (BC) aerosol, emitted from incomplete combustion, may be the second strongest positive anthropogenic climate forcing following carbon dioxide, which drew attention for potential climate mitigation from reducing BC emissions (Jacobson, 2004; Shindell et al., 2012; Bond et al., 2013; Smith and Mizrahi, 2013). The relationship between forcing and surface temperature changes caused by BC is complex and forcing is not a reliable indicator of the climatic impact of BC emissions (Stjern et al., 2017). BC absorbs solar radiation within the atmospheric column thereby warming the atmosphere with an influence on surface temperature that depends on its vertical location. At high altitudes, BC cools the surface by absorbing solar radiation (i.e., blocking it from reaching the surface) (Ramanathan and Carmichael, 2008), while BC at low altitudes warms the surface through diabatic heating (Ban-Weiss et al., 2012). In addition, heating the atmosphere and cooling the surface can increase atmospheric stability and therefore affect cloud formation, lifetime, and dynamical processes (Koren et al., 2004; McFarquhar and Wang, 2006; Koch and Del Genio, 2010). Through transformation from hydrophobic aggregates to hydrophilic particles coated with water-soluble substances (*i.e.,* aging processes), BC can become cloud-nucleating particles (Oshima et al., 2009), alter cloud microphysical processes, and suppress precipitation (Boucher et al., 2013). BC-induced warming or cooling can increase or decrease surface evaporation, resulting in further changes in precipitation and cloud formation (McFarquhar and Wang, 2006; Andrews et al., 2010; Ming et al., 2010; Ban-Weiss et al., 2012; Kvalevåg et al., 2013). BC can also decrease surface albedo through deposition on snow and ice, which is especially important to the climate at high latitudes and, particularly the Arctic (Flanner et al., 2007; Qian et al., 2014) as snow/ice-albedo effects are

Deleted: attentions

strong there. Taken together, these processes result in interactions between BC and the atmosphere that can ultimately alter the net impact of BC on climate, which have been termed rapid adjustments (Stjern et al., 2017).

Studies found that increases in BC emissions may contribute to the amplification of Arctic warming directly by absorbing solar radiation in the atmosphere and indirectly by reducing surface albedo through deposition on snow and ice (Flanner et al., 2007; Qian et al., 2014). Flanner (2013) highlighted the importance of BC vertical location in Arctic climate responses, with surface warming (cooling) due to BC in the lower (upper) troposphere. In addition, BC outside the Arctic can influence the Arctic climate through changing poleward heat transport. With BC snow/ice-albedo effect excluded, Shindell and Faluvegi (2009) modeled an Arctic surface warming (cooling) due to reducing (enhancing) mid-latitude BC atmospheric concentrations. Sand et al. (2013a) found that this was due to the increased northward heat transport into the Arctic. However, in another study where BC emissions were perturbed instead of concentrations, Sand et al. (2013b) reported a decrease in northward heat transport due to increases in mid-latitude BC emissions and suggested that the heating effect of BC transported to the Arctic dominated the Arctic heating in the mid-latitude perturbation simulation, leading to the opposite direction of atmospheric heat transport compared to the concentration-driven perturbations. They also found that increases in both BC emission and BC concentration in the Arctic atmosphere may weaken poleward heat transport due to increasing Arctic temperature driven by BC heating in the atmosphere and on snow and ice surfaces. Therefore, understanding the Arctic climate impact of regional BC emissions is important for the Arctic climate mitigation (Sand et al., 2016).

In order to archive a statistically significant signal for Arctic surface temperature responses to

Deleted: of

BC emissions, Sand et al. (2013b) scaled present-day BC emissions within the Arctic by a factor of 150 and emissions from mid-latitudes by a factor of 9, respectively, in the NorESM model with BC snow/ice-albedo effects included. They found that emissions of BC within the Arctic have an Arctic surface temperature response 5 times larger than those from mid-latitudes and attributed this to BC snow/ice-albedo feedbacks. The impact of BC emission perturbations on mid-latitudes were not examined in that study, which we do in this work to contrast the impact of BC on the Arctic with mid-latitudes.

Much of the previous work on BC has used atmosphere-only models or prescribed BC concentrations (Hansen et al., 2005; Ming et al., 2010; Ban-Weiss et al., 2012; Sand et al., 2013a), which artificially reduces variability in model results. Results qualitatively differ between prescribed BC-concentration and emission-driven simulations with coupled models (Sand et al., 2013a,b, 2015). A previous study using coupled models found that the BC response in three of these models showed high variability and inconsistency in the net sign of the responses to present-day BC emissions both between models and even between ensemble members from the same model (Baker et al., 2015). Stjern et al. (2017) investigated climate responses to a tenfold increase in present-day anthropogenic BC concentrations or emissions using five concentration-driven and four emission-driven global climate models. They found that low-level cloud amounts increase, while higher-level clouds are diminished for all models, which is dominated by rapid adjustments. The negative rapid adjustments from changing clouds dampened positive instantaneous radiative forcing of BC at the TOA, leading to a relatively small global surface warming. However, this study did not consider response variability or non-linearity of responses. We note that the model used in our study contains a different aerosol treatment

Deleted: it

Deleted: ours

(see below) than the model used in Stjern et al. (2015).

To better understand the impacts of BC on climate, we present a comprehensive analysis using a set of coupled simulations that examine regional climate responses, non-linearity, and short-term transient climate responses to BC emission perturbations. We focus in particular on the Arctic and also variability to assess if climate responses to BC emission changes are likely to be discernable. Only combustion and process-based anthropogenic BC emissions are perturbed, given that the net global climate impact of open burning emissions has been assessed to be small due to their high organic carbon fraction. A summary of key results is provided below.

2. Methods

2.1 Model description

Here we use the fully coupled CESM (Community Earth System Model; Hurrell et al., 2013) to simulate climate responses to BC emission perturbations. In CAM5-MAM4 (Community Atmosphere Model version 5), the atmospheric component of CESM, mass and number concentrations of aerosols are predicted within four lognormal modes (i.e., Aitken, accumulation, coarse, and primary carbon mode) of the modal aerosol module (MAM4; Liu et al., 2016). BC is emitted into the primary-carbon mode and aged into the accumulation mode when coated with sulfate or secondary organic aerosol. Particles in the accumulation mode, including BC and other species, can serve as cloud condensation nuclei and have microphysical effects on stratiform clouds and precipitation. The model physically treats aerosol-cloud interactions using two-moment stratiform cloud microphysics, which predicts number concentrations and mixing ratios of cloud water and ice (Morrison and Gettelman, 2008; Gettelman et al., 2010). Activation of

stratiform cloud droplets is based on the scheme of Abdul-Razzak and Ghan (2000). In addition to the standard treatments of aerosol-cloud interactions, we also include a set of modifications that improves the simulation of aerosol wet scavenging and convective transport (Wang et al., 2013). Although aerosols have no microphysical impact on convective clouds, BC induced atmospheric heating can affect the ambient temperature and convection. Convective precipitation can scavenge and remove aerosols. Previous studies have extensively evaluated the CAM5 model simulations of concentration, deposition, vertical profile and optical properties of BC (Wang et al., 2013; Wang et al., 2015; Zhang et al., 2015a,b; Liu et al., 2016; Yang et al., 2017, 2018a,b)), as well as climate variables (Hurrell et al., 2013; Yang et al., 2016a,b). The model can simulate well the BC aerosol and climate variables in most regions of the globe, but was reported to underestimate BC concentrations over China (Yang et al., 2018a) and the Arctic (Wang et al., 2013) (although this earlier study used a different emissions dataset), implying a possible underestimate of climate responses to BC emissions in this study.

In our model simulations, atmospheric radiative transfer is calculated twice with BC included and excluded, respectively. The changes in direct radiative effect and cloud radiative effect induced by BC perturbation are calculated as $\Delta(F_{clear} - F_{clear,clean})$ and $\Delta(F_{clean} - F_{clear,clean})$, respectively, where F_{clear} is the TOA flux calculated neglecting scattering and absorption by clouds, F_{clean} is the TOA flux calculated neglecting scattering and absorption by BC, $F_{clear,clean}$ is the TOA flux calculated neglecting scattering and absorption by both clouds and BC, and Δ refers to the differences between the control and one of the emission perturbed simulations (Ghan, 2013). Note that these quantities include the impact of slow responses and feedbacks (e.g., changes in sea surface temperature and sea ice and feedbacks with clouds) so are not strictly comparable to

Deleted: The CAM5 model has been

Deleted: in simulating

Deleted: in previous studies

Deleted:).

the conventional definition of radiative forcing (Boucher et al., 2013). The BC snow/ice-albedo effect on top of land and sea ice is included in the model (Flanner et al., 2007; Yang et al., 2017, 2018c).

2.2 Experimental configuration and emissions

Deleted: configurations

The following simulations are performed in this study. All insolation, greenhouse gas concentrations and aerosol and precursor emissions, except BC, are fixed at year 1850 levels, which include open burning emissions (van Marle et al., 2017).

The MID7X and ARC150X simulations use large emission perturbations to result in signals large enough for detailed analysis. These regions are also particularly important for BC impacts on the Arctic. The multipliers were selected following Sand et al. (2013b) with the expectation that these would result in similar radiative perturbations. This also allows a direct comparison to these previous results (Sand et al., 2013b; and also Baker et al., 2015), which are also BC-emission simulations using a coupled model with snow/ice-albedo feedbacks. The PD simulation then allows us to evaluate the impact of present-day anthropogenic emissions. In brief, the simulations conducted are:

1. PD: control simulation for BC in present-day conditions. BC emissions are fixed at year 2010 (average of 2008–2012).
2. ARC150X: perturbed simulation to quantify the climate responses to Arctic BC emissions. Same as PD except that year 2010 level anthropogenic BC emissions over the Arctic (60–90°N) are scaled by a factor of 150.

3. MID7X: perturbed simulation to quantify the climate responses to mid-latitude BC emissions. Same as PD except that year 2010 level anthropogenic BC emissions over the mid-latitudes (28–60°N) are scaled by a factor of 7.

4. ARC75X: perturbed simulation to quantify non-linearity of climate responses to Arctic BC emissions. Same as ARC150X except that Arctic BC emissions are scaled by a factor of 75.

5. MID3.5X: perturbed simulation to quantify non-linearity of climate responses to mid-latitude BC emissions. Same as MID7X except that mid-latitude BC emissions are scaled by a factor of 3.5.

6. MID14X: perturbed simulation to quantify non-linearity of climate responses to mid-latitudes BC emissions. Same as MID7X except that mid-latitude BC emissions are scaled by a factor of 14.

7. PI: sensitivity simulation for BC in preindustrial conditions to compare results with Baker et al. (2015). BC emissions are at year 1850 levels.

Both mass and number of BC emissions are perturbed proportionally. Each simulation has one ensemble member for 100 years which are branched from year 81 of the PI simulation after 80 years spin-up, with the last 80 years used for most analysis. Another four short-term ensemble members for 30 years are conducted under both ARC150X and MID7X to examine the short-term transient climate response to BC emissions. These are branched from years 96, 112, 120, and 140 of PI simulation.

The CEDS (Community Emissions Data System) anthropogenic emissions (Hoesly et al., 2018) (version 2017-05-18) that were developed for the CMIP6 (Coupled Model Intercomparison

Project Phase 6) model experiments are used in our simulations. Note that this emission dataset includes monthly BC emission seasonality, which has been shown to be important for simulating BC in the Arctic (Stohl et al., 2013). Figure S1 shows spatial distribution of annual anthropogenic BC emissions for year 2010 (average of 2008–2012) and the regions for BC emission perturbation. Over 60–90°N, anthropogenic BC emissions are mostly over the lower latitude of the Arctic (60–70°N). Over the mid-latitudes, high BC emissions are mainly located over eastern China. The annual total anthropogenic BC emission from the Arctic in year 2010 is 0.08 Tg C yr^{-1}, with 70% contributed by energy sector. Scaled by a factor of 150, ARC150X has 12.63 Tg C yr^{-1} more BC emissions than the PD in the Arctic. About 3.46 Tg C yr^{-1} of BC is emitted from the mid-latitudes, with the largest contribution from the residential sector (36%). With a scaling factor of 7, MID7X includes an additional 20.74 Tg C yr^{-1} of BC emission from mid-latitudes, as compared to PD. Global annual anthropogenic BC for PD is 7.72 Tg C yr^{-1}, much higher than 0.92 Tg C yr^{-1} for PI.

3. Regional climate responses to increases in Arctic and mid-latitude BC emissions

We first examine results from simulations with large perturbations of Arctic and mid-latitude BC emissions (ARC150X and MID7X). Our initial simulations focused on these regions due to the potentially high sensitivity of the Arctic to BC emissions. Figure 1 presents the increases in annual, zonal-mean BC concentrations from ARC150X and MID7X simulations, as compared to PD. Both Arctic and mid-latitude BC emissions lead to BC concentration increases in the entire Northern Hemisphere, with Arctic emissions mainly impacting low altitudes within the Arctic. In ARC150X, due to extremely low temperatures at the surface and therefore temperature inversions and a

Deleted: both

transport barrier (so called Arctic front), BC concentration increases are mainly located over low altitudes within the Arctic. In MID7X, increased mid-latitude emissions produce large increases in BC concentrations between 30°–45°N. BC emitted over the mid-latitudes, which is lifted above the boundary layer and transported at higher altitudes into the Arctic, leading to increased concentrations of BC in the Arctic atmosphere. This spatial pattern is similar to that in Sand et al. (2013b).

To explore the importance of emissions from these source regions to BC column burdens, Table 1 summarizes BC burden efficiency, which is defined as the changes in regional mean column burden of BC produced by per unit emission change, calculated by differences between the perturbed and PD simulation. Over the Arctic, increases in Arctic local BC emissions lead to an Arctic column burden efficiency of 0.425 ±0.024 mg m^{-2} (Tg yr^{-1})$^{-1}$. The burden efficiency of mid-latitude emissions over the mid-latitudes is 0.191 ±0.004 mg m^{-2} (Tg yr^{-1})$^{-1}$, less than half of the efficiency of Arctic emission on Arctic burden due to lower precipitation and frequent temperature inversion in the Arctic compared to mid-latitudes. While the relative impact of mid-latitude emissions on the Arctic burden efficiency (0.106 ±0.004 mg m^{-2} (Tg yr^{-1})$^{-1}$) is smaller than either of the above efficiencies, the 28 times larger present-day total emissions from mid-latitudes (3.70 Tg yr^{-1}) than the Arctic (0.13 Tg yr^{-1}) dominate column burden contributions.

Table 1 also summarizes the changes in BC direct radiative effect, cloud radiative effect, and snow/ice-albedo forcing induced by these large BC perturbations. Note that these values include feedback effects from the coupled system, so are not comparable to conventionally defined radiative forcing values. The albedo change due to BC deposition on snow and ice is responsible for a significant increase in Arctic surface forcing in both perturbations, with far smaller changes

Deleted: increasing BC concentrations

Deleted: those

Deleted: additional

Deleted: different

Deleted: the increase in

Deleted: a

Deleted: simulation

Deleted: 30

Deleted: are likely to

per unit emission in mid-latitudes. Positive changes in direct radiative effect are offset by negative changes in cloud radiative effect from increases in low cloud in the Arctic and decreases in mid-level and high cloud over the mid-latitudes, similar to previous results with a tenfold increase in present-day anthropogenic BC emissions (Stjern et al., 2017).

Forcing efficiencies for direct radiative effect, cloud radiative effect and snow/ice-albedo forcing (i.e., forcings produced by per unit emission change) are also summarized in Table 1. Over the Arctic, local emissions from the Arctic have 2–4 times higher forcing efficiencies than emissions from the mid-latitudes, suggesting higher impacts of a unit Arctic BC emission change to Arctic energy balance. Over the mid-latitudes, although forcing efficiencies for direct radiative and cloud radiative effects for Arctic emissions are 2–3 times lower than mid-latitude emissions, the snow/ice-albedo forcing efficiencies are similar between Arctic and mid-latitude emissions.

The annual mean surface air temperature response in ARC150X shows a significant warming over both the Arctic and mid-latitudes (Figure 2). MID7X shows temperature increases over the Arctic and most of the mid-latitude land regions, while surface temperature decreases over some oceanic and coastal areas. The presence of areas with both surface warming and cooling decreases the net average temperature change over mid-latitudes. The seasonal mean surface air temperature responses present similar spatial patterns (Figure S2), but slightly different magnitudes (Figure S3). Over the Arctic, the warming due to Arctic BC emissions is weakest in boreal summer. This is because the smaller summer sea ice and snow fraction in the Arctic weakens BC snow/ice-albedo forcing. However, in the mid-latitudes, warming is strongest in boreal summer for both Arctic and mid-latitude BC emissions, because of stronger summer solar insolation and, therefore, stronger BC heating in the atmosphere.

Deleted: of

Deleted: of

Deleted: effect

Deleted: effect

Deleted: responses

Deleted: show

Due to the increased atmospheric absorption from BC, northward heat transport for both perturbations decreases (Figure 3), consistent in sign with the results of Sand et al. (2013b). The increases in temperature but decreases in net northward heat transport indicate that the heating induced by changes in BC direct radiative effect and BC snow/ice-albedo forcing dominate the overall BC-induced changes in energy balance over the Arctic and mid-latitudes.

Arctic emissions are more efficient at impacting Arctic surface air temperatures with an Arctic temperature sensitivity to Arctic emissions (0.169 ±0.052 K (Tg yr^{-1})$^{-1}$) seven times as large as the Arctic temperature sensitivity to mid-latitude emissions (0.023 ±0.038 K (Tg yr^{-1})$^{-1}$). Mid-latitude emissions, however, are likely to have a larger present-day impact overall due to their 35 times larger preindustrial to present-day emission increase (2.874 Tg yr^{-1}) than Arctic emissions (0.082 Tg yr^{-1}). Note that, the Arctic temperature sensitivities are about 30% and 50% smaller than those found in the coupled NorESM model experiments of Sand et al. (2013b) for Arctic and mid-latitude emission perturbation simulations, respectively, probably due to different model parameterizations and/or different vertical profile of BC driving the net effect of BC impact on Arctic surface temperature (Flanner, 2013).

The vertical distribution of annual, zonal mean temperature responses (Figure 4) shows that the ARC150X leads to a strong warming from the surface to 400 hPa over the Arctic and between 40°–60°N. In MID7X, although the zonal mean surface temperature response is relatively weak compared to ARC150X, a significant warming is found in mid-latitudes between 500 and 200 hPa. BC transported from mid-latitudes into the Arctic at high altitudes also results in Arctic temperature increases aloft, between 400 and 300 hPa.

These changes in temperature pattern can change the stability of the atmosphere and impact

Deleted: 30

Deleted: levels.

Deleted: over the Arctic.

atmospheric circulation, as shown in Figure 5. Increases in BC emissions over both the Arctic and mid-latitudes exert anomalous upward motions in the Arctic and downward motions over the mid-latitudes, but for different reasons. In ARC150X, stronger warming at the Arctic surface, compared to high altitudes, likely due to the BC snow/ice-albedo effect, produces anomalous upward motions in the Arctic and compensating downward motions between 50°–60°N. In MID7X, the stronger BC warming at higher altitudes in mid-latitudes increases atmospheric stability and leads to strong anomalous downward motions between 40°–60°N and compensating upward motions over the Arctic and 10°–30°N (Johnson et al., 2004). Increasing surface temperature and anomalous upward motion over the Arctic can weaken the Arctic front, and the anomalous downward motion over the mid-latitudes favors air stagnation.

Because of the anomalous downward motions over mid-latitudes in both ARC150X and MID7X, high and/or mid-level cloud fraction decrease over mid-latitudes (Figure 6). Due to slow feedbacks from increases in surface temperature in the Arctic (Figure 2) and decreases in snow and sea ice, low cloud fraction increases in the Arctic for both ARC150X and MID7X. The increases in low cloud over mid-latitude oceans, which cause the cooling noted above, are due to rapid adjustments as free-tropospheric BC heating reduces mixing with dry air above the BC layer and increases the amount of marine stratocumulus (Johnson et al., 2004; Sand et al., 2013a; Stjern et al., 2017).

Figure 7 shows changes in the total precipitation rate for the perturbed simulations. Increases in Arctic and mid-latitude BC emissions lead to significant decreases in precipitation over 60°N and 30–50°N, respectively, in correspondence with anomalous downward motions (Figure 5) and decreases in mid-level and high clouds (Figure 6) over these regions. Averaged over the Arctic

Deleted: .¶

Deleted: shows changes in annual mean meridional circulation.

Deleted: the

Deleted: that the

and mid-latitudes, changes in precipitation are weak, compared to uncertainties, except for the mid-latitude precipitation response to BC emitted from mid-latitudes. The mid-latitude precipitation sensitivity is –7.67 (±3.34) μm day^{-1} (Tg yr^{-1})$^{-1}$ for MID7X. Another feature of the precipitation response is related to a northward shift in the ITCZ (Intertropical Convergence Zone) in MID7X, which is consistent with the hemispherically asymmetric warming pattern driven by increases in mid-latitude BC emissions (Hwang et al., 2013; Baker et al., 2015).

Both ARC150X and MID7X show significant decreases by 13% and 3%, respectively, in fractional area covered by sea ice over the Arctic, as compared to PD (Figure S4). The snow depth over land also decreases, especially over Greenland. The water equivalent snow depth averaged over Arctic land decreases by 5.0 cm (27% relative to PD) and 0.8 cm (4%), respectively, for ARC150X and MID7X.

4. Non-linearity of climate responses.

We also evaluated the linearity of these responses by testing different emission perturbation sizes. Figure 8 shows burden efficiencies, temperature and precipitation sensitivities from simulations with Arctic BC emissions scaled by 75 and 150, respectively, and mid-latitude BC emissions scaled by 3.5, 7 and 14, respectively, with values summarized in Table 2. Stronger emission perturbations have a higher burden efficiency. Over the Arctic, this is caused by anomalous Arctic upward motions that weaken the Arctic front, lifting BC higher and leading to a longer BC lifetime together with easier transport into the Arctic (Figure S5). Over mid-latitudes, anomalous mid-latitude downward motions favor stagnation, which in turn accumulates more BC in the atmosphere, together with decrease in precipitation (and wet removal rate), contributing to

Deleted: S2

Deleted: and Table 2

Deleted: these values

Deleted: S3

increases in burden efficiency. All differences in burden efficiencies between simulations with different emission perturbation sizes are statistically significant with 95% confidence.

Despite this higher burden efficiency, the efficiency (per unit emission) of the direct radiative effect decreases slightly. This is because strong BC perturbations lead to more BC suspended in the atmosphere. More BC increases the attenuation of the transmitted radiation, leading to a decrease in efficiency of BC light absorption in the lower atmosphere and leading to a lower efficiency of direct radiative effect for a stronger BC emissions perturbation.

The temperature sensitivity is lower, with 95% significance, for stronger emission perturbations for both mid-latitude and Arctic BC, between ARC75X and ARC150X, as well between MID7X and MID14X (Table 2). The BC snow/ice-albedo effect is found to be the most important factor in influencing Arctic temperature (Sand et al., 2013b). Larger temperature increases from stronger BC emission perturbations speed up sea ice and snow melt, leading to a weaker annual mean snow/ice-albedo effect per unit BC emission for both Arctic and mid-latitudes. Therefore, the BC snow/ice-albedo effect is more efficient for weaker emission perturbations, i.e., 0.151 (±0.011) vs. 0.099 (±0.006) (W m^{-2} (Tg yr^{-1})$^{-1}$) for ARC75X and ARC150X and 0.026 (±0.002) vs. 0.020 (±0.002) (W m^{-2} (Tg yr^{-1})$^{-1}$) for MID7X and MID14X of Arctic BC snow/ice-albedo forcing efficiencies. All snow/ice-albedo forcing efficiency differences are statistically significant. Together with lower efficiency of the direct radiative effect, these explain the lower temperature sensitivity for stronger emission perturbation. The non-linearity in snow-ice feedback relative to emissions size appears to be the primary driver of surface temperature response non-linearity in these results.

Additional evidence for BC non-linearity can be found in the literature. Sand et al. (2015)

Deleted: of

Deleted: .

simulated climate responses to BC in NorESM with present-day emissions multiplied by 25 and reported that the changes in TOA net shortwave flux was 7.5 (±0.3) W m^{-2} relative to preindustrial conditions and the temperature response was 1.2 (±0.1) K. If we assume a linear emission-response relationship, present-day BC would cause an inferred shortwave flux and surface temperature change of 0.312 (±0.013) W m^{-2} and 0.050 (±0.004) K in Sand et al. (2015), much lower than the 0.552 W m^{-2} and 0.141 K found in Baker et al. (2015) for a present-day BC emission perturbation with essentially the same model. Note that the change in shortwave flux is not proportional to the surface temperate change, further emphasizing that forcing is not a good predictor of surface temperature change for BC. This comparison is consistent with our finding that temperature sensitivity is lower for stronger BC emission perturbations. We note, however, that emission datasets with different spatial distributions and seasonality were used in those two experiments (because of this the difference in global emissions between the two experiments is about 17, not 25 times). While this might impact the magnitude of model responses, it is unlikely to change the overall conclusion of a substantially different temperature response to current-day emissions as compared to a 17–25 times larger BC perturbation.

The mid-latitude shows significantly stronger precipitation sensitivity for a stronger perturbation, comparing MID7X and MID14X, which is consistent with the higher burden efficiency. This is in the opposite direction to the surface temperature sensitivity. Variability in MID3.5X is larger than the mean value for both temperature and precipitation sensitivity, which highlights the challenge of testing differences for smaller BC perturbation magnitudes. Note that the impact of BC on clouds and precipitation is uncertain, especially in the Arctic, due to the limited treatment of Arctic clouds in climate models (McFarquhar et al., 2011). These results suggest that in order to

Deleted: changes

Deleted: .

Deleted: perturbation.

Deleted: a

examine the climate responses to BC emissions in short-term climate model simulations, a large emission perturbation is needed to get a clear signal, but non-linearity of the responses also needs to be evaluated.

5. Short-term transient climate responses

To assess the short-term transient climate responses to BC emissions, Figure 9 shows surface temperature responses to BC emissions from ARC150X and MID7X for the first 30 years averaged over five short ensemble members. We also show a numerical fit to the short-term transient response using a Hamiltonian Monte Carlo technique (Betancourt, 2017). We fit to the following form:

$$T_{ave}\,(1 - e^{-t/\tau}),$$

where we have constrained the fit to converge to the long-term average temperature response (T_{ave}) by our finding that there is no detectable long-term trend after the initial transient period over a 100-year time horizon.

Over both the Arctic and mid-latitudes, transient temperature responses quickly approach a quasi-equilibrium state. Transient timescales (τ) for the ARC150X perturbation were estimated to be 2.7 (2.0, 3.4) years, while the mid-latitude timescales for the ARC150X and MID7X perturbations were 1.8 (1.1, 2.2) and 2.9 (1.2, 4.2) years respectively (brackets provide 10-90% fitting intervals). The Arctic response to MID7X was too noisy to produce a fit. These timescales are shorter than those in a global BC perturbation experiment (Sand et al., 2015), which is expected as ocean thermal inertia would play a larger role globally as compared to the Northern Hemisphere or Arctic. The BC response timescales here are also shorter than those seen from

Deleted: /τ)

Deleted: observation

Deleted: provide

Deleted: not only

CO_2 concentration steps in GCMs (Geoffroy et al., 2013). There is also no long-term temperature increase, at least over a 100-year time horizon, after the initial transient period. A linear fit over years 10-100 for the perturbation responses results in no statistically significant linear trends for any of the four perturbations (see SI code).

Note that the average of even five ensemble members shows oscillatory behavior due to the imposition of a step BC emission perturbation. This oscillatory behavior degrades our ability to quantify the perturbation response timescale. In future work, a linearly phased-in perturbation might result in a cleaner signal for determining the initial response time-scale.

6. Climate responses to present-day anthropogenic BC emissions

Baker et al. (2015) showed that the climate responses to BC emissions had very large uncertainties based on results from four global models. Here, we also quantified the impact of present-day anthropogenic BC emissions (Figure 10) by comparing a present-day (PD) and pre-industrial (PI) simulation conducted with the CESM-CAM5-MAM4 model used in this work. PD emissions produce statistically significant surface air temperature changes over only limited regions in the Northern Hemisphere. Decreased temperatures are found over eastern China, South Asia, North Atlantic Ocean, and North American Arctic, partly due to cloud changes driven by BC rapid adjustments. Increased temperatures are found over the Tibetan Plateau, Greenland and high-latitude land regions likely because of the BC snow/ice-albedo effect (Figure S6).

The spatial pattern is similar to that from the ECHAM6-HAM2 in Baker et al. (2015). Although CESM-CAM5-MAM4 also includes the BC snow/ice-albedo effect, we do not see the strong warming produced in NorESM under present-day BC emissions. In Baker et al. (2015), NorESM

Deleted: changes in

Deleted: concentrations

Deleted:), but there

Deleted: In future work, a

Deleted: S4

had a global net TOA shortwave forcing efficiency of 0.076 W m^{-2} (Tg yr^{-1})$^{-1}$, nominally higher than 0.043 ±0.073 W m^{-2} (Tg yr^{-1})$^{-1}$ calculated in this study with CESM-CAM5-MAM4, although the difference is well within one standard deviation. Longer model runs would be needed to determine if the BC snow/ice-albedo effect is significantly different in CESM and NorESM. In addition, there may be a small contribution from a shorter BC lifetime (7.22 days in CESM-CAM5-MAM4 Vs. 7.82 days in NorESM) that might also help explain the weaker warming in CESM-CAM5-MAM4 as compared to NorESM.

We find that variability is substantial in our experiments. Although statistically significant surface temperature changes are found regionally, as mentioned above, large-scale global surface temperature change from current-day BC emissions is statistically indistinguishable from zero (0.006 ±0.238 K globally and 0.020 ±0.346 K for land only). The global temperature response is within the range of –0.085 to 0.152 K from the four models in Baker et al. (2015). Even in the large MID7X perturbation, variability is still fairly large relative to the signal (0.45 ±0.27 K for mid-latitude temperate change) and would overwhelm any large-scale signal for more realistic perturbation sizes. Similarly, while the mid-latitude precipitation response to mid-latitude BC emissions is strong for a MID7X perturbation, this would be difficult to detect for a present-day perturbation.

Deleted: Large-scale

7. Conclusions and discussions

BC has been estimated to potentially have one of the largest positive (warming) anthropogenic forcing influences. As a result, there has been substantial scientific and policy attention focused on the potential for BC to moderate climate change in the near-term. In this

study, for the first time, we conduct a comprehensive set of emission-driven experiments using a leading coupled climate model (CESM). With a comprehensive set of experiments, we examined regional climate responses, non-linearity, and short-term transient responses to BC emission perturbations in the Arctic, mid-latitudes, and globally.

With increases in mid-latitude BC emissions, surface air temperature increases over land, while it decreases over oceanic and coastal areas. Increases in Arctic BC emissions lead to warming over both the Arctic and mid-latitudes. Increases in Arctic and mid-latitude BC emissions also decrease precipitation over 60°N and 30–50°N, respectively. Arctic emissions are more efficient in influencing Arctic surface air temperatures compared to mid-latitude emissions, with an Arctic temperature sensitivity to Arctic emissions seven times as large as that to mid-latitude emissions.

We find that climate responses do not scale linearity with emissions. While stronger BC emission perturbations have a higher burden efficiency, efficiencies of snow/ice-albedo forcing and direct radiative effect are lower, leading to a lower temperature sensitivity for stronger BC emission perturbations.

BC also impacts temperature much faster than greenhouse gas forcing, with transient temperature responses in the Arctic and mid-latitudes approaching a quasi-equilibrium state with a timescale of 2–3 years. While it has previously been found that, globally, aerosols have a faster impact on temperature as compared to greenhouse gases (Shindell., 2014), termed a "geometric effect" (Meinshausen et al., 2011), we find here that BC perturbations have a very short response time, particularly for Arctic and mid-latitude perturbations. This means that previous studies which have implicitly assumed that the temperature response timescales of BC and GHGs are the same

Deleted: a significant

Deleted: Climate

Deleted: perturbation.

(Boucher and Reddy 2008, Stohl et al., 2015) have likely underestimated the short-term impact of BC emission changes.

We find large variability in BC-induced climate changes. Baker et al. (2015) provided error bars of global temperature response for different models in their Figure 4a. We note, however, that the error bars in Baker et al. are underestimated because of their assumption of independence of all annual data points (note their use of 1σ/sqrt(N) in their error bars for Figure 4). Climate model surface temperatures are strongly correlated over short time scales, which means that instead of the number of data points, a more appropriate measure is the effective number of independent data points (N_{eff}). The 100-year model runs examined here do not provide enough data for this calculation. (Note that we were able to estimate N_{eff} for the 300-year CESM control run from CMIP5, which indicates that runs around 3 times as long as those presented here may be necessary). We, therefore, present standard deviation as a metric of variance.

The standard deviation (SD) of global mean surface temperature in PI, PD, and in all of our perturbed simulations is around 0.17–0.19 K, indicating that the dominant source of temperature variability is probably due to internal climate variability or model noise. The SD for temperature responses in perturbed simulations relative to PD are in ranges of 0.24–0.26, roughly 1.4 times the control run temperature variability. This is in the expectation from subtracting two independent Gaussian noise distributions. While there could be an additional contribution to variability from BC-climate interactions, this appears to be small in this case given the relatively small surface temperature response to BC. We also observe large variability in cloud radiative effects, which we note may be impacted by interactions with BC.

While we have demonstrated non-linear responses at high emission levels, this non-linearity

Deleted: model

Deleted: of their study

is not sufficient to produce statistically significant global temperature changes from present-day BC emissions in this model. Such non-linearities mean that the implications of large BC emission perturbation experiments, such as recent tenfold BC experiments (Stjern et al., 2017) for present-day conditions are unclear. While snow/ice-albedo feedbacks appear to dominate the non-linear relationship in these results, this may not be the case in other models.

Our results point to the importance of better quantifying the variability in BC responses in the Earth system. We note that in the one model with a consistent PD-PI signal in a set of recent PD-PI BC experiments (NorESM1-M), the size of that signal is still smaller than the variability found here, based on similar SD in Arctic temperature change for the ARC150X simulations in the two models (compare Figure S3 here with Figure 9 in Sand et al. (2013b)). If the global variability of BC response in NorESM is also similar to that in CESM, then the global average temperature change from NorESM (0.141 K) (Baker et al., 2015) is also much smaller than the SD in CESM of 0.238 K. However, we do note that there was a fair degree of consistency in temperature change signal in NorESM between two ensemble members (0.129 K and 0.152 K). This may mean that variability in the global BC response in the NorESM model could be smaller than seen in our results due to the stronger NorESM BC temperature response. Longer simulations would likely be required to assess this. While, compared to temperature or precipitation, aerosol burdens, BC direct radiative effects and snow/ice-albedo forcings have much larger signal to noise ratios, i.e. ratio of mean response to standard deviation (Table 1), and can be useful as diagnostics, BC forcing does not provide a reliable indicator of surface temperature changes across models.

These results indicate that even substantial BC emissions reductions from current levels may lead to detectable surface temperature changes for only limited regions of the globe. Our results

Deleted: experiments[5]

Deleted: S5

have significant implications for near-term climate mitigation associated with BC as well as global and regional climate attribution. We note that regional climate sensitivities (RCS), used as an approximate approach to represent the impact of BC (Collins et al., 2013; Sand et al., 2016), are generally evaluated using model simulations with prescribed forcing or burdens (Shindell and Faluvegi, 2009), which artificially reduce response variability and imply a certainty in BC responses that may not exist in reality. Variability within any given model run, which has generally not been reported in current literature, is large relative to BC responses. It is, therefore, not clear if current BC emission levels result in statistically significant large-scale climatic changes. We suggest that impacts of BC on climate should be expressed directly in terms of impacts per unit emissions (e.g. Table 1), and not only relative to forcing, given the complex relationship between BC climatic impacts and top of the atmosphere forcing. In addition, BC impacts should be re-evaluated using coupled models, and provided with measures of response variability, such as standard deviation. In order to better assess the potential impact of changes in BC emissions it is critical to quantify the non-linearity of BC response efficiencies with respect to emission perturbation size in other models, as well as the causes of those non-linearities.

Deleted: ,

Acknowledgments.

This research is based on work that was supported by the U.S. Environmental Protection Agency, and the U.S. Department of Energy (DOE), Office of Science, Biological and Environmental Research as part of the Regional and Global Climate Modeling program. The Pacific Northwest

Deleted: Climate Change Division of

National Laboratory is operated for DOE by Battelle Memorial Institute under contract DE-AC05-76RLO1830. The National Energy Research Scientific Computing Center (NERSC) provided computational support. Model results are available through NERSC upon request.

References

Abdul-Razzak, H. and Ghan, S. J.: A parameterization of aerosol activation 2. Multiple aerosol types, J. Geophys. Res., 105, 6837–6844, doi:10.1029/1999JD901161, 2000.

Andrews, T., Forster, P. M., Boucher, O., Bellouin, N., and Jones, A.: Precipitation, radiative forcing and global temperature change, Geophys. Res. Lett., 37, L14701, doi:10.1029/2010GL043991, 2010.

Baker, L. H., Collins, W. J., Olivié, D. J. L., Cherian, R., Hodnebrog, Ø., Myhre, G., and Quaas, J.: Climate responses to anthropogenic emissions of short-lived climate pollutants, Atmos. Chem. Phys., 15, 8201-8216, doi:10.5194/acp-15-8201-2015, 2015.

Ban-Weiss, G. A., Cao, L., Bala, G., and Caldeira, K.: Dependence of climate forcing and response on the altitude of black carbon aerosols, Clim. Dyn., 38, 897–911, doi:10.1007/s00382-011-1052-y, 2012.

Betancourt, M.: A conceptual introduction to Hamiltonian Monte Carlo, arXiv preprint, arXiv:1701.02434, 2017.

Bond, T. C., Doherty, S. J., Fahey, D. W., Forster, P. M., Berntsen, T., DeAngelo,B. J., Flanner, M. G., Ghan, S., Kärcher, B., Koch, D., Kinne, S., Kondo, Y., Quinn, P. K., Sarofim, M. C., Schultz, M. G., Schulz, M., Venkataraman, C., Zhang, H., Zhang, S., Bellouin, N., Guttikunda, S. K., Hopke, P. K., Jacobson, M. Z., Kaiser, J. W., Klimont, Z., Lohmann, U., Schwarz, J. P., Shindell, D., Storelvmo, T., Warren, S. G., and Zender, C. S.: Bounding the role of black carbon in the climate system: A scientific assessment, J. Geophys. Res., 118, 5380–5552, doi:10.1002/jgrd.50171, 2013.

Boucher, O., Randall, D., Artaxo, P., Bretherton, C., Feingold, G., Forster, P., Kerminen, V.-M., Kondo, Y., Liao, H., Lohmann, U., Rasch, P., Satheesh, S. K., Sherwood, S., Stevens, B., and Zhang, X. Y.: Clouds and Aerosols, in: Climate Change 2013: The Physical Science Basis, Contribution of Working Group I to the Fifth Assessment Report of the Intergovernmental Panel on Climate Change, edited by: Stocker, T. F., Qin, D., Plattner, G.-K., Tignor, M., Allen, S. K., Boschung, J., Nauels, A., Xia, Y., Bex, V., and Midgley, P. M., Cambridge University Press, Cambridge, United Kingdom and New York, NY, USA, 571–658, doi:10.1017/CBO9781107415324.016, 2013.

Boucher, O. and Reddy, M. S.: Climate trade-off between black carbon and carbon dioxide emissions, Energ. Policy, 36, 193–200, doi:10.1016/j.enpol.2007.08.039, 2008.

Collins, W. J., Fry, M. M., Yu, H., Fuglestvedt, J. S., Shindell, D. T., and West, J. J.: Global and regional temperature-change potentials for near-term climate forcers, Atmos. Chem. Phys., 13, 2471-2485, https://doi.org/10.5194/acp-13-2471-2013, 2013.

635 Flanner, M. G.: Arctic climate sensitivity to local black carbon, J. Geophys. Res. Atmos., 118,
636 1840–1851, doi:10.1002/jgrd.50176, 2013.
637
638 Flanner, M. G., Zender, C. S., Randerson, J. T., and Rasch, P. J.: Present day climate forcing and
639 response from black carbon in snow, J. Geophys. Res., 112, D11202,
640 doi:10.1029/2006JD008003, 2007.
641
642 Geoffroy, O., Saint-Martin, D., Bellon, G., Voldoire, A., Olivié, D. J., and Tytéca, S.: Transient
643 climate response in a two-layer energy-balance model. Part II: Representation of the efficacy
644 of deep-ocean heat uptake and validation for CMIP5 AOGCMs, J. Climate, 26, 1859–1876,
645 doi:10.1175/JCLI-D-12-00196.1, 2013.
646
647 Gettelman, A., Liu, X., Ghan, S. J., Morrison, H., Park, S., Conley, A. J., Klein, S. A., Boyle, J.,
648 Mitchell, D. L., and Li, J. L. F.: Global simulations of ice nucleation and ice supersaturation
649 with an improved cloud scheme in the Community Atmosphere Model, J. Geophys. Res., 115,
650 D18216, doi:10.1029/2009jd013797, 2010.
651
652 Ghan, S. J.: Technical Note: Estimating aerosol effects on cloud radiative forcing, Atmos. Chem.
653 Phys., 13, 9971–9974, doi:10.5194/acp-13-9971-2013, 2013.
654
655 Hansen, J., Sato, M., Ruedy, R., Nazarenko, L., Lacis, A., Schmidt, G. A., Russell, G., Aleinov, I.,
656 Bauer, M., Bauer, S., Bell, N., Cairns, B., Canuto, V., Chandler, M., Cheng, Y., Del Genio, A.,
657 Faluvegi, G., Fleming, E., Friend, A., Hall, T., Jackman, C., Kel- ley, M., Kiang, N., Koch, D.,
658 Lean, J., Lerner, J., Lo, K., Menon, S., Miller, R., Minnis, P., Novakov, T., Oinas, V., Perlwitz,
659 Ja., Perlwitz, Ju., Rind, D., Romanou, A., Shindell, D., Stone, P., Sun, S., Tausnev, N.,
660 Thresher, D., Wielicki, B., Wong, T., Yao, M., and Zhang, S.: Efficacy of climate forcings, J.
661 Geophys. Res., 110, D18104, doi:10.1029/2005JD005776, 2005.
662
663 Hoesly, R. M., Smith, S. J., Feng, L., Klimont, Z., Janssens-Maenhout, G., Pitkanen, T., Seibert, J.
664 J., Vu, L., Andres, R. J., Bolt, R. M., Bond, T. C., Dawidowski, L., Kholod, N., Kurokawa, J.-I.,
665 Li, M., Liu, L., Lu, Z., Moura, M. C. P., O'Rourke, P. R., and Zhang, Q.: Historical (1750–2014)
666 anthropogenic emissions of reactive gases and aerosols from the Community Emissions
667 Data System (CEDS), Geosci. Model Dev., 11, 369–408, doi:10.5194/gmd-11-369-2018,
668 2018.
669
670 Hurrell, J. W., Holland, M. M., Gent, P. R., Ghan, S., Kay, J. E., Kushner, P. J., Lamarque, J. F.,
671 Large, W. G., Lawrence, D., Lindsay, K., Lipscomb, W. H., Long, M. C., Mahowald, N., Marsh,
672 D. R., Neale, R. B., Rasch, P., Vavrus, S., Vertenstein, M., Bader, D., Collins, W. D., Hack, J.
673 J., Kiehl, J., and Marshall, S.: The Community Earth System Model A Framework for
674 Collaborative Research, B. Am. Meteorol. Soc., 94, 1339–1360,
675 doi:10.1175/BAMS-D-12-00121.1, 2013.
676
677 Hwang, Y.-T., Frierson, D. M. W., and Kang, S. M.: Anthropogenic sulfate aerosol and the
678 southward shift of tropical precipitation in the late 20th century, Geophys. Res. Lett., 40,

679 2845–2850, doi:10.1002/grl.50502, 2013.
680
681 Jacobson, M. Z.: Climate response of fossil fuel and biofuel soot, accounting for soot's feedback
682 to snow and sea ice albedo and emissivity, J. Geophys. Res., 109, D21201,
683 doi:10.1029/2004JD004945, 2004.
684
685 Johnson, B. T., Shine, K. P., and Forster, P. M.: The semi-direct aerosol effect: Impact of
686 absorbing aerosols on marine stratocumulus, Q. J. Roy. Meteor. Soc., 130, 1407–1422,
687 doi:10.1256/qj.03.61, 2004.
688
689 Koch, D. and Del Genio, A. D.: Black carbon semi-direct effects on cloud cover: review and
690 synthesis, Atmos. Chem. Phys., 10, 7685-7696, doi:10.5194/acp-10-7685-2010, 2010.
691
692 Koren, I., Kaufman, Y. J., Remer, L. A., and Martins, J. V.: Measurement of the effect of Amazon
693 smoke on inhibition of cloud formation, Science, 303, 1342–1345, doi:
694 10.1126/science.1089424, 2004.
695
696 Kvalevåg, M. M., Samset, B. H., and Myhre, G.: Hydrological sensitivity to greenhouse gases and
697 aerosols in a global climate model, Geophys. Res. Lett., 40, 1432–1438,
698 doi:10.1002/grl.50318, 2013.
699
700 Liu, X., Ma, P.-L., Wang, H., Tilmes, S., Singh, B., Easter, R. C., Ghan, S. J., and Rasch, P. J.:
701 Description and evaluation of a new four-mode version of the Modal Aerosol Module (MAM4)
702 within version 5.3 of the Community Atmosphere Model, Geosci. Model Dev., 9, 505–522,
703 doi:10.5194/gmd-9-505-2016, 2016.
704
705 McFarquhar, G. M., Ghan, S., Verlinde, J., Korolev, A., Strapp, J. W., Schmid, B., Tomlinson, J. M.,
706 Wolde, M., Brooks, S. D., Cziczo, D., Dubey, M. K., Fan, J., Flynn, C., Gultepe, I., Hubbe, J.,
707 Gilles, M. K., Laskin, A., Lawson, P., Leaitch, W. R., Liu, P., Liu, X., Lubin, D., Mazzoleni, C.,
708 Macdonald, A.-M., Moffet, R. C., Morrison, H., Ovchinnikov, M., Shupe, M. D., Turner, D. D.,
709 Xie, S., Zelenyuk, A., Bae, K., Freer, M., and Glen, A.: Indirect and Semi-Direct Aerosol
710 Campaign (ISDAC): The Impact of Arctic Aerosols on Clouds, B. Am. Meteorol. Soc., 92,
711 183–201, doi:10.1175/2010BAMS2935.1, 2011.
712
713 McFarquhar, G. M. and Wang, H.: Effects of Aerosols on Trade Wind Cumuli over the Indian
714 Ocean: Model Simulations, Q. J. R. Meteorol. Soc., 132, 821–843, doi:10.1256/qj.04.179,
715 2006.
716
717 Meinshausen, M., Smith, S. J., Calvin, K., Daniel, J. S., Kainuma, M. L. T., Lamarque, J.-F.,
718 Matsumoto, K., Montzka, S. A., Raper, S. C. B., Riahi, K., Thomson, A., Velders, G. J. M., and
719 van Vuuren, D. P. P.: The RCP greenhouse gas concentrations and their extensions from
720 1765 to 2300, Climatic Change, 109, 213–241, doi:10.1007/s10584-011-0156-z, 2011.
721
722 Ming, Y., Ramaswamy, V., and Persad, G.: Two opposing effects of absorbing aerosols on

723 global-mean precipitation, Geophys. Res. Lett., 37, L13701, doi:10.1029/2010GL042895,
724 2010.
725
726 Morrison, H. and Gettelman, A.: A new two-moment bulk stratiform cloud microphysics scheme in
727 the Community Atmosphere Model, version 3 (CAM3), Part I: Description and numerical tests,
728 J. Clim., 21, 3642–3659, doi:10.1175/2008JCLI2105.1, 2008.
729
730 Oshima, N., Koike, M., Zhang, Y., Kondo, Y., Moteki, N., Takegawa, N., and Miyazaki, Y.: Aging of
731 black carbon in outflow from anthropogenic sources using a mixing state resolved model:
732 Model development and evaluation, J. Geophys. Res., 114, D06210, doi:
733 10.1029/2008JD010680, 2009.
734
735 Qian, Y., Wang, H., Zhang, R., Flanner, M. G., and Rasch, P. J.: A sensitivity study on modeling
736 black carbon in snow and its radiative forcing over the Arctic and Northern China, Environ.
737 Res. Lett., 9, 064001, doi:10.1088/1748-9326/9/6/064001, 2014.
738
739 Ramanathan, V. and Carmichael, G.: Global and regional climate changes due to black carbon,
740 Nat. Geosci., 1, 221–227, doi:10.1038/ngeo156, 2008.
741
742 Sand, M., Berntsen, T. K., Kay, J. E., Lamarque, J. F., Seland, Ø., and Kirkevåg, A.: The Arctic
743 response to remote and local forcing of black carbon, Atmos. Chem. Phys., 13, 211-224,
744 doi:10.5194/acp-13-211-2013, 2013a.
745
746 Sand, M., Berntsen, T. K., Seland, Ø., and Kristjánsson, J. E.: Arctic surface temperature change
747 to emissions of black carbon within Arctic or midlatitudes, J. Geophys. Res. Atmos., 118,
748 7788–7798, doi:10.1002/jgrd.50613, 2013b.
749
750 Sand, M., Iversen, T., Bohlinger, P., Kirkevåg, A., Seierstad, I., Seland, Ø., and Sorteberg, A: A
751 standardized global climate model study showing unique properties for the climate response
752 to black carbon aerosols, J. Climate., 28, 2512–2526, doi:10.1175/JCLI-D-14-00050.1, 2015.
753
754 Sand, M., Berntsen, T. K., von Salzen, K., Flanner, M. G., Langner, J., and Victor, D. G.:
755 Response of Arctic temperature to changes in emissions of short-lived climate forcers, Nat.
756 Clim. Change, 6, 286–289, doi:10.1038/nclimate2880, 2016.
757
758 Shindell, D.: Inhomogeneous forcing and transient climate sensitivity, Nat. Clim. Change, 4, 274–
759 277, doi:10.1038/nclimate2136, 2014.
760
761 Shindell, D. and Faluvegi, G.: Climate response to regional radiative forcing during the twentieth
762 century, Nat. Geosci., 2, 294–300, doi:10.1038/ngeo473, 2009.
763
764 Shindell, D., Kuylenstierna, J. C. I., Vignati, E., van Dingenen, R., Amann, M., Klimont, Z.,
765 Anenberg, S. C., Muller, N., Janssens-Maenhout, G., Raes, F., Schwartz, J., Faluvegi, G.,
766 Pozzoli, L., Kupiainen, K., Höglund-Isaksson, L., Emberson, L., Streets, D., Ramanathan, V.,

Hicks, K., Oanh, N. T. K., Milly, G., Williams, M., Demkine, V., and Fowler, D.: Simultaneously Mitigating Near-Term Climate Change and Improving Human Health and Food Security, Science, 335, 183–189, doi:10.1126/science.1210026, 2012.

Smith, S. J. and Mizrahi, A.: Near-term climate mitigation by short-lived forcers, Proc. Natl. Acad. Sci., 110, 14202–14206, doi:10.1073/pnas.1308470110, 2013.

Stjern, C. W., Samset, B. H., Myhre, G., Forster, P. M., Hodnebrog, Ø., Andrews, T., Boucher, O., Faluvegi, G., Iversen, T., Kasoar, M., Kharin, V., Kirkevåg, A., Lamarque, J.-F., Olivieì, D., Richardson, T., Shawki, D., Shindell, D., Smith, C., Takemura, T., and Voulgarakis, A.: Rapid adjustments cause weak surface temperature response to increased black carbon concentrations, J. Geophys. Res. Atmos., 122, 11462–11481, doi:10.1002/2017JD027326, 2017.

Stohl, A., Aamaas, B., Amann, M., Baker, L. H., Bellouin, N., Berntsen, T. K., Boucher, O., Cherian, R., Collins, W., Daskalakis, N., Dusinska, M., Eckhardt, S., Fuglestvedt, J. S., Harju, M., Heyes, C., Hodnebrog, Ø., Hao, J., Im, U., Kanakidou, M., Klimont, Z., Kupiainen, K., Law, K. S., Lund, M. T., Maas, R., MacIntosh, C. R., Myhre, G., Myriokefalitakis, S., Olivié, D., Quaas, J., Quennehen, B., Raut, J.-C., Rumbold, S. T., Samset, B. H., Schulz, M., Seland, Ø., Shine, K. P., Skeie, R. B., Wang, S., Yttri, K. E., and Zhu, T.: Evaluating the climate and air quality impacts of short-lived pollutants, Atmos. Chem. Phys., 15, 10529–10566, doi:10.5194/acp-15-10529-2015, 2015.

Stohl, A., Klimont, Z., Eckhardt, S., Kupiainen, K., Shevchenko, V. P., Kopeikin, V. M., and Novigatsky, A. N.: Black carbon in the Arctic: the underestimated role of gas flaring and residential combustion emissions, Atmos. Chem. Phys., 13, 8833–8855, doi:10.5194/acp-13-8833-2013, 2013.

van Marle, M. J. E., Kloster, S., Magi, B. I., Marlon, J. R., Daniau, A.-L., Field, R. D., Arneth, A., Forrest, M., Hantson, S., Kehrwald, N. M., Knorr, W., Lasslop, G., Li, F., Mangeon, S., Yue, C., Kaiser, J. W., and van der Werf, G. R.: Historic global biomass burning emissions for CMIP6 (BB4CMIP) based on merging satellite observations with proxies and fire models (1750–2015), Geosci. Model Dev., 10, 3329–3357, doi:10.5194/gmd-10-3329-2017, 2017.

Wang, H., Easter, R. C., Rasch, P. J., Wang, M., Liu, X., Ghan, S. J., Qian, Y., Yoon, J.-H., Ma, P.-L., and Vinoj, V.: Sensitivity of remote aerosol distributions to representation of cloud–aerosol interactions in a global climate model, Geosci. Model Dev., 6, 765-782, doi:10.5194/gmd-6-765-2013, 2013.

Wang, M., Larson, V., Ghan, S., Ovchinnikov, M., Schanen, D., Xiao, H., Liu, X., Guo, Z., and Rasch, P.: A multiscale modeling framework model (superparameterized CAM5) with a higher-order turbulence closure: Model description and low-cloud simulations, J. Adv. Model. Earth Syst., 7, 484–509, doi:10.1002/2014MS000375, 2015.

Yang, Y., Russell, L. M., Xu, L., Lou, S., Lamjiri, M. A., Somerville, R. C. J., Miller, A. J., Cayan, D. R., DeFlorio, M. J., Ghan, S. J., Liu, Y., Singh, B., Wang, H., Yoon, J.-H., and Rasch, P. J.: Impacts of ENSO events on cloud radiative effects in preindustrial conditions: Changes in cloud fraction and their dependence on interactive aerosol emissions and concentrations, J. Geophys. Res. Atmos., 121, 6321–6335, doi:10.1002/2015JD024503, 2016a.

Yang, Y., Russell, L. M., Lou, S., Lamjiri, M. A., Liu, Y., Singh, B., and Ghan, S. J.: Changes in Sea Salt Emissions Enhance ENSO Variability, J. Climate, 29, 8575–8588, doi:10.1175/JCLI-D-16-0237.1, 2016b.

Yang, Y., Wang, H., Smith, S. J., Ma, P.-L., and Rasch, P. J.: Source attribution of black carbon and its direct radiative forcing in China, Atmos. Chem. Phys., 17, 4319-4336, doi:10.5194/acp-17-4319-2017, 2017.

Yang, Y., Wang, H., Smith, S. J., Zhang, R., Lou, S., Qian, Y., Ma, P.-L., Rasch, P. J.: Recent intensification of winter haze in China linked to foreign emissions and meteorology, Sci. Rep., 8, 2107, doi:10.1038/s41598-018-20437-7, 2018a.

Yang, Y., Wang, H., Smith, S. J., Zhang, R., Lou, S., Yu, H., Li, C., and Rasch, P. J.: Source apportionments of aerosols and their direct radiative forcing and long-term trends over continental United States, Earth's Future, 6, 793–808, doi:10.1029/2018EF000859, 2018b.

Yang, Y., Wang, H., Smith, S. J., Easter, R. C., and Rasch, P. J.: Sulfate aerosol in the Arctic: Source attribution and radiative forcing, J. Geophys. Res. Atmos., 123, 1899–1918, doi:10.1002/2017JD027298, 2018c.

Zhang, R., Wang, H., Hegg, D. A., Qian, Y., Doherty, S. J., Dang, C., Ma, P.-L., Rasch, P. J., and Fu, Q.: Quantifying sources of black carbon in western North America using observationally based analysis and an emission tagging technique in the Community Atmosphere Model, Atmos. Chem. Phys., 15, 12805-12822, doi:10.5194/acp-15-12805-2015, 2015a.

Zhang, R., Wang, H., Qian, Y., Rasch, P. J., Easter, R. C., Ma, P.-L., Singh, B., Huang, J., and Fu, Q.: Quantifying sources, transport, deposition, and radiative forcing of black carbon over the Himalayas and Tibetan Plateau, Atmos. Chem. Phys., 15, 6205-6223, doi:10.5194/acp-15-6205-2015, 2015b.

Table 1. Changes in black carbon (BC) column burden, direct radiative effect (DRE) and cloud radiative effect (CRE) at the top of the atmosphere (TOA), surface BC snow/ice-albedo forcing, surface temperature (T) and total precipitation rate (P, including rain and snow) averaged over the Arctic (60–90°N), mid-latitudes (28–60°N) and the globe between perturbed (ARC150X/MID7X) and PD simulations. BC burden, DRE, CRE, and snow/ice-albedo forcing efficiencies, T sensitivity and P sensitivity are calculated as changes in regional mean BC column burden, DRE, CRE, snow/ice-albedo forcing, T and P divided by changes in global total BC emissions between perturbed and PD simulations, respectively. 1-σ for 80-annual means is shown in the parentheses. Note that these quantities include the impact of slow responses and feedbacks (e.g., changes in sea surface temperature and sea ice and feedbacks with clouds) so are not strictly comparable to the conventional definition of radiative forcing.

	ΔColumn Burden (mg m^{-2})			Burden Eff. (mg m^{-2} (Tg yr^{-1})$^{-1}$)			ΔDRE (W m^{-2})		
	60–90°N	28–60°N	Global	60–90°N	28–60°N	Global	60–90°N	28–60°N	Global
ARC150X	5.37 (±0.30)	1.34 (±0.05)	0.63 (±0.03)	0.425 (±0.024)	0.106 (±0.004)	0.050 (±0.002)	3.94 (±0.39)	0.83 (±0.04)	0.45 (±0.03)
MID7X	2.19 (±0.09)	3.97 (±0.09)	1.26 (±0.03)	0.106 (±0.004)	0.191 (±0.004)	0.061 (±0.001)	2.90 (±0.19)	2.49 (±0.09)	1.00 (±0.04)
	DRE Eff. (W m^{-2} (Tg yr^{-1})$^{-1}$)			ΔCRE (W m^{-2})			CRE Eff. (W m^{-2} (Tg yr^{-1})$^{-1}$)		
	60–90°N	28–60°N	Global	60–90°N	28–60°N	Global	60–90°N	28–60°N	Global
ARC150X	0.39 (±0.03)	0.11 (±0.00)	0.05 (±0.00)	–3.83 (±0.98)	–0.46 (±0.84)	–0.22 (±0.54)	–0.30 (±0.08)	–0.04 (±0.07)	–0.02 (±0.04)
MID7X	0.17 (±0.01)	0.22 (±0.01)	0.08 (±0.00)	–2.30 (±0.96)	–3.16 (±0.90)	–1.26 (±0.51)	–0.11 (±0.05)	–0.15 (±0.04)	–0.06 (±0.02)
	ΔSnow/ice-albedo Forcing (W m^{-2})			Snow/ice-albedo Eff. (W m^{-2} (Tg yr^{-1})$^{-1}$)			ΔT (K)		
	60–90°N	28–60°N	Global	60–90°N	28–60°N	Global	60–90°N	28–60°N	Global
ARC150X	1.26 (±0.08)	0.12 (±0.02)	0.10 (±0.01)	0.099 (±0.006)	0.010 (±0.002)	0.008 (±0.001)	2.13 (±0.65)	0.78 (±0.22)	0.48 (±0.26)
MID7X	0.53 (±0.05)	0.18 (±0.03)	0.07 (±0.01)	0.026 (±0.002)	0.009 (±0.001)	0.003 (±0.000)	0.48 (±0.79)	0.45 (±0.27)	0.23 (±0.26)
	T Sensitivity (K (Tg yr^{-1})$^{-1}$)			ΔP (mm day^{-1})			P Sensitivity (μm day^{-1} (Tg yr^{-1})$^{-1}$)		
	60–90°N	28–60°N	Global	60–90°N	28–60°N	Global	60–90°N	28–60°N	Global
ARC150X	0.169 (±0.052)	0.062 (±0.018)	0.038 (±0.020)	–0.043 (±0.079)	–0.011 (±0.066)	0.010 (±0.023)	–3.38 (±6.29)	–0.86 (±5.26)	0.77 (±1.84)
MID7X	0.023 (±0.038)	0.022 (±0.013)	0.011 (±0.012)	0.048 (±0.096)	–0.159 (±0.069)	–0.032 (±0.022)	2.34 (±4.61)	–7.67 (±3.34)	–1.52 (±1.04)

Table 2. BC burden, DRE, CRE, and snow/ice-albedo forcing efficiencies, T sensitivity and P sensitivity over the Arctic (60–90°N), mid-latitudes (28–60°N) and the globe between perturbed (ARC75X/ARC150X/MID3.5X/MID7X/MID14X) and PD simulations. 1-σ for 80-annual means is shown in the parentheses. Bold values between two simulations (ARC75X/ARC150X, MID3.5X/MID7X, and MID7X/MID14X) indicates statistically significant changes with 95% confidence from a two-tailed Student's t test.

	ARC75X	ARC150X	MID3P5X	MID7X	MID14X
	Burden Eff. (mg m^{-2} (Tg yr^{-1})$^{-1}$)				
60–90°N	**0.406 (±0.021)**	**0.425 (±0.024)**	**0.095 (±0.005)**	**0.106 (±0.004)**	**0.124 (±0.004)**
28–60°N	**0.097 (±0.004)**	**0.106 (±0.004)**	**0.175 (±0.005)**	**0.191 (±0.004)**	**0.219 (±0.005)**
Global	**0.047 (±0.002)**	**0.050 (±0.002)**	**0.055 (±0.001)**	**0.061 (±0.001)**	**0.070 (±0.002)**
	DRE Eff. (W m^{-2} (Tg yr^{-1})$^{-1}$)				
60–90°N	**0.346 (±0.036)**	**0.312 (±0.031)**	**0.146 (±0.014)**	**0.140 (±0.009)**	**0.137 (±0.006)**
28–60°N	**0.069 (±0.005)**	**0.066 (±0.003)**	**0.129 (±0.006)**	**0.120 (±0.004)**	**0.112 (±0.003)**
Global	**0.038 (±0.003)**	**0.035 (±0.003)**	**0.051 (±0.003)**	**0.048 (±0.002)**	**0.046 (±0.001)**
	CRE Eff. (W m^{-2} (Tg yr^{-1})$^{-1}$)				
60–90°N	**–0.533 (±0.232)**	**–0.303 (±0.078)**	–0.091 (±0.166)	**–0.111 (±0.046)**	**–0.015 (±0.029)**
28–60°N	0.010 (±0.222)	–0.037 (±0.067)	**0.070 (±0.203)**	**–0.152 (±0.043)**	**0.129 (±0.035)**
Global	**–0.028 (±0.071)**	**–0.017 (±0.043)**	0.013 (±0.058)	**–0.061 (±0.025)**	**0.035 (±0.010)**
	Snow/ice-albedo Eff. (W m^{-2} (Tg yr^{-1})$^{-1}$)				
60–90°N	**0.151 (±0.011)**	**0.099 (±0.006)**	**0.030 (±0.003)**	**0.026 (±0.002)**	**0.020 (±0.002)**
28–60°N	**0.013 (±0.003)**	**0.010 (±0.002)**	**0.011 (±0.002)**	**0.009 (±0.001)**	**0.007 (±0.001)**
Global	**0.012 (±0.001)**	**0.008 (±0.001)**	**0.004 (±0.001)**	**0.003 (±0.000)**	**0.003 (±0.000)**
	T Sensitivity (K (Tg yr^{-1})$^{-1}$)				
60–90°N	**0.239 (±0.116)**	**0.169 (±0.052)**	0.042 (±0.098)	**0.023 (±0.038)**	**0.008 (±0.015)**
28–60°N	0.067 (±0.032)	0.062 (±0.018)	0.020 (±0.025)	**0.022 (±0.013)**	**0.015 (±0.005)**
Global	**0.040 (±0.035)**	**0.038 (±0.020)**	0.008 (±0.033)	**0.011 (±0.012)**	**0.005 (±0.005)**
	P Sensitivity (μm day-1 (Tg yr^{-1})$^{-1}$)				
60–90°N	–2.88 (±13.39)	–3.38 (±6.29)	1.73 (±10.85)	2.34 (±4.61)	1.86 (±2.06)
28–60°N	–0.96 (±9.45)	–0.86 (±5.26)	–7.69 (±8.90)	**–7.67 (±3.34)**	**–8.53 (±1.61)**
Global	0.31 (±3.10)	0.77 (±1.84)	–1.99 (±2.81)	–1.52 (±1.04)	–2.15 (±0.49)

Figures for Paper

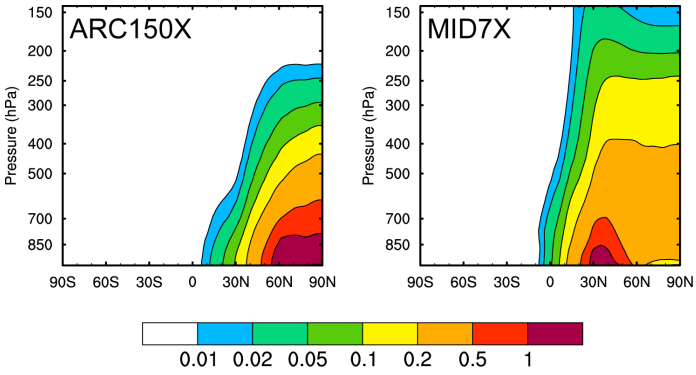

Figure 1. Difference in annual and zonal mean BC concentrations (μg m^{-3}) between ARC150X (left)/MID7X (right) and PD simulations.

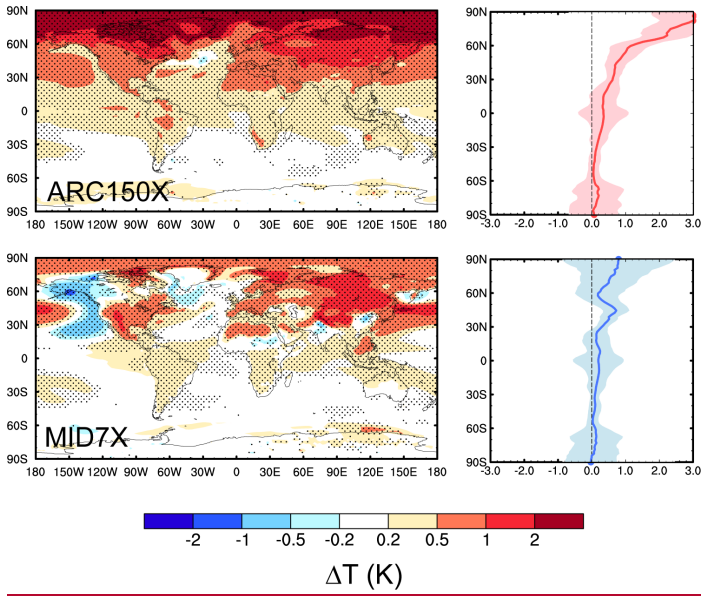

Figure 2. Spatial distribution (left) and zonal mean (right) of changes in annual mean surface air temperature (K) for ARC150X (top) and MID7X (bottom) compared to PD. The dotted areas in left panels indicate statistical significance with 95% confidence from a two-tailed Student's t test.

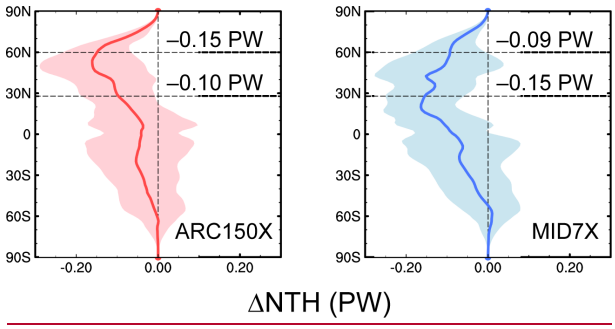

Figure 3. Zonal mean of changes in annual mean northward heat transport (NHT, PW) for ARC150X (left) and MID7X (right) compared to PD. Values of changes in NHT across 60°N and 28°N are shown in each panel. The shaded areas represent 1-σ for 80-annual means.

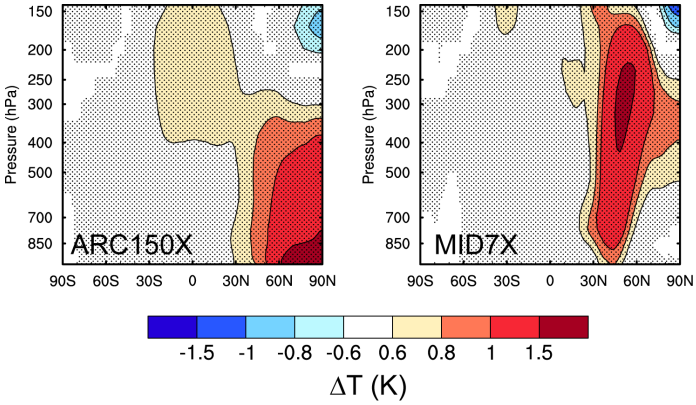

Figure 4. Changes in annual and zonal mean temperature (K) for ARC150X (left) and MID7X (right) compared to PD. The dotted areas indicate statistical significance with 95% confidence from a two-tailed Student's t test.

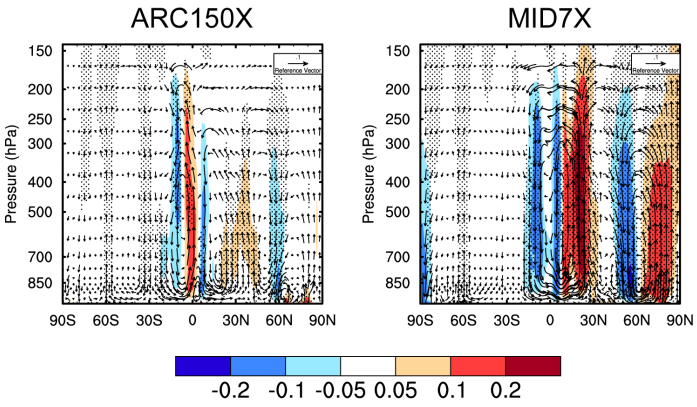

Figure 5. Changes in annual and zonal mean meridional wind vectors (m s^{-1}) and vertical velocity (contours; Pa s^{-1} scaled by a factor of –100) for ARC150X (left) and MID7X (right) compared to PD. The dotted areas indicate statistical significance with 95% confidence from a two-tailed Student's t test.

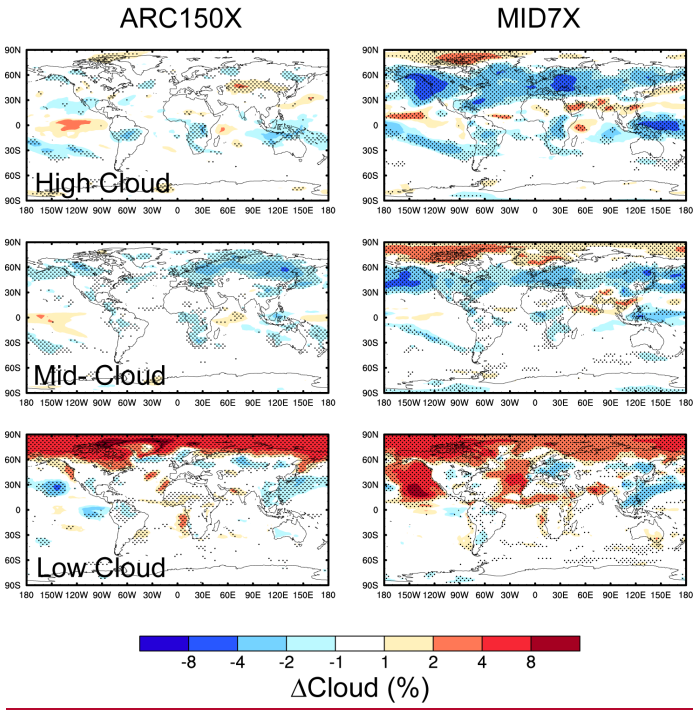

Figure 6. Changes in annual mean high (top), mid-level (middle), and low (bottom) cloud fraction (%) for ARC150X (left) and MID7X (right) compared to PD. The dotted areas indicate statistical significance with 95% confidence from a two-tailed Student's t test.

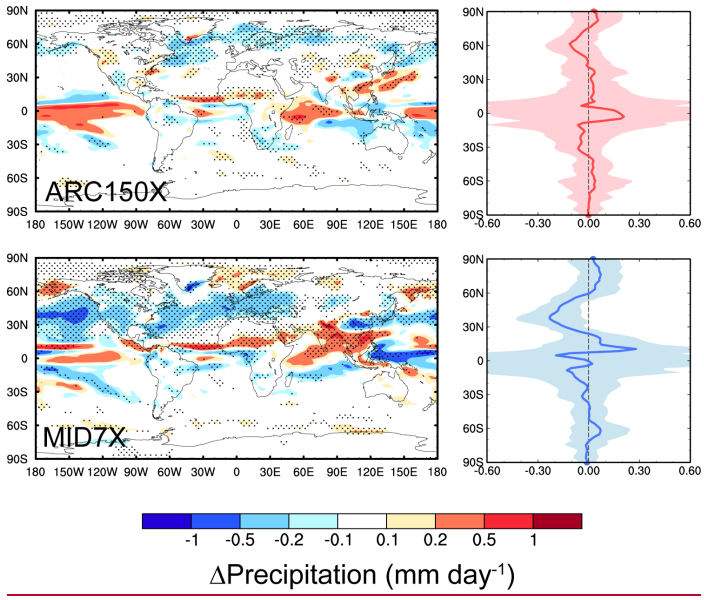

Figure 7. Spatial distribution (left) and zonal mean (right) of changes in annual mean total precipitation rate (mm day^{-1}) for ARC150X (top) and MID7X (bottom) compared to PD. The dotted areas in left panels indicate statistical significance with 95% confidence from a two-tailed Student's t test.

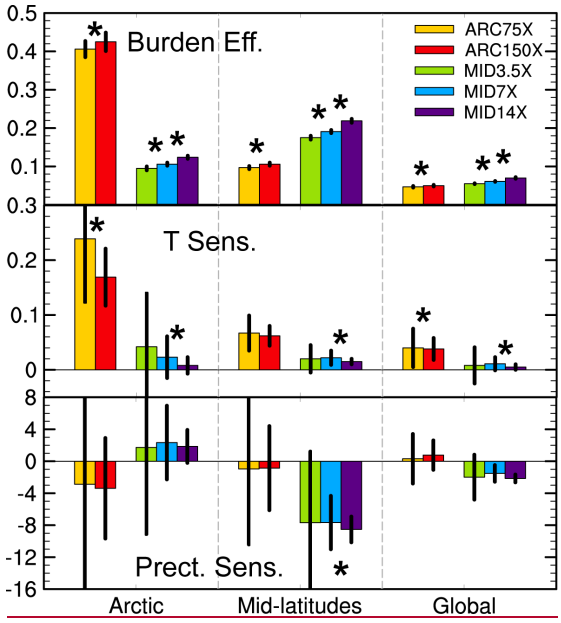

Figure 8. Burden efficiencies, temperature and precipitation sensitivities over the Arctic, mid-latitudes and the whole globe for ARC75X, ARC150X, MID3.5X, MID7X and MID14X. Burden efficiencies, temperature sensitivity and precipitation sensitivity are calculated as changes in regional mean BC column burden, surface temperature and total precipitation rate divided by changes in global total BC emissions between perturbed and PD simulations, respectively. Error bars represent 1-σ for 80-annual means. Asterisk between two bars (ARC75X/ARC150X, MID3.5X/MID7X, and MID7X/MID14X) indicates statistically significant changes with 95% confidence from a two-tailed Student's t test.

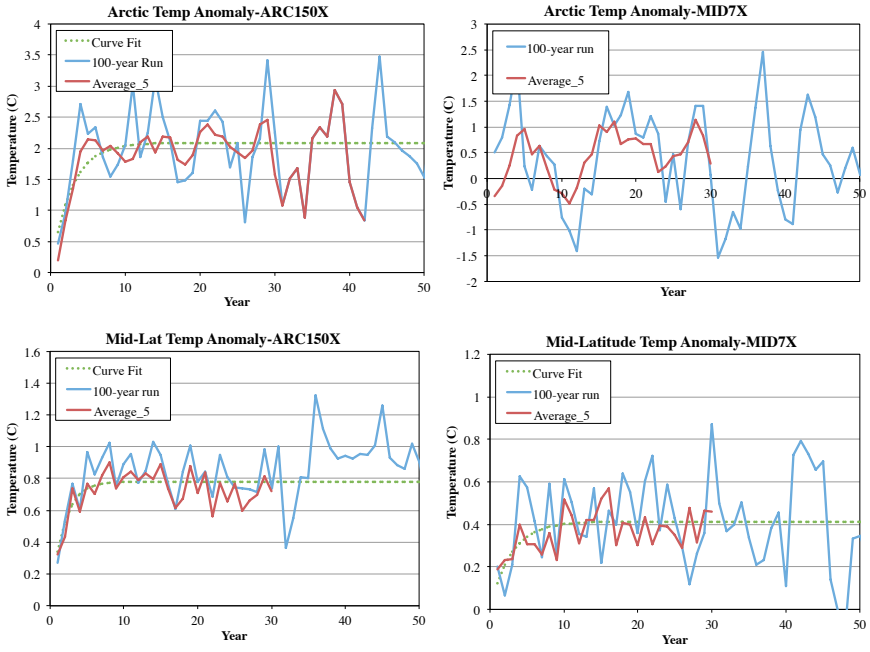

Figure 9. Time series of mean surface temperature response from ARC150X (left) and MID7X (right) BC emission perturbations as compared to PD. The response is shown over the Arctic (top) and mid-latitudes (bottom). Shown are the 100-year ensemble simulation (blue lines), the average of five 30-year ensemble members (red), and a numerical fit for an exponential approach to the long-term average (green dashed line). Curve fits used the package STAN in R, which is Bayesian inference using the No-U-Turn sampler. Note that MID7X Arctic temperature response does not result in a fit due to noise.

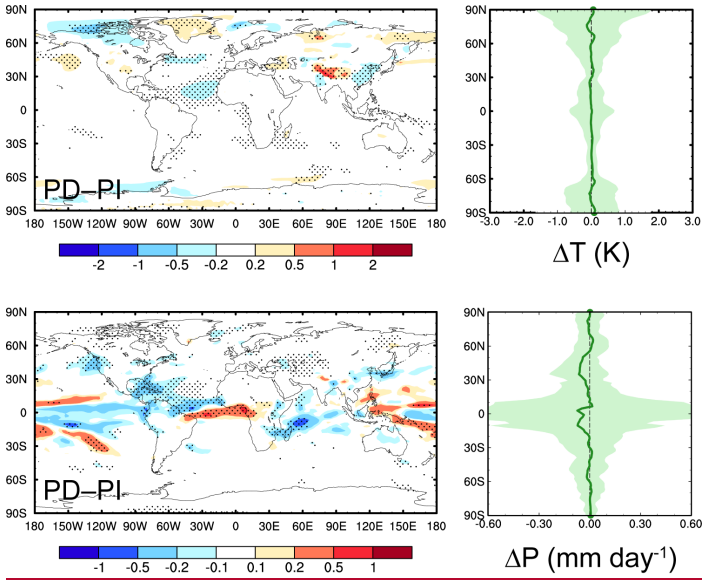

Figure 10. Spatial distribution (left) and zonal mean (right) of differences in annual mean surface temperature (K, top) and total precipitation rate (mm day^{-1}, bottom) between PD and PI. The dotted areas in left panels indicate statistical significance with 95% confidence from a two-tailed Student's t test.